Adaptive and Intelligent Digital Signal Processing for Improved Optical Interconnection

SUN Lin[1], DU Jiangbing[1], HUA Feng[2], TANG Ningfeng[2], HE Zuyuan[1]

(1. State Key Laboratory of Advanced Optical Communication Systems and Networks, Shanghai Jiao Tong University, Shanghai 200240, China;
2. State Key Laboratory of Mobile Network and Mobile Multimedia Technology, ZTE Corporation, Shenzhen, Guangdong 518055, China)

DOI: 10.12142/ZTECOM.202002008

http://kns.cnki.net/kcms/detail/34.1294.TN.20200612.1034.001.html, published online June 12, 2020

Manuscript received: 2019-03-04

Abstract: In recent years, explosively increasing data traffic has been boosting the continuous demand of high speed optical interconnection inside or among data centers, high performance computers and even consumer electronics. To pursue the improved interconnection performance of capacity, energy efficiency and simplicity, effective approaches are demonstrated including particularly advanced digital signal processing (DSP) methods. In this paper, we present a review about the enabling adaptive DSP methods for optical interconnection applications, and a detailed summary of our recent and ongoing works in this field. In brief, our works focus on dealing with the specific issues for short-reach interconnection scenarios with adaptive operation, including signal-to-noise-ratio (SNR) limitation, level nonlinearity distortion, energy efficiency consideration and the decision precision.

Keywords: optical interconnection; digital signal processing; advanced modulation formats

Citation (IEEE Format): L. Sun, J. B. Du, F. Hua, et al., "Adaptive and intelligent digital signal processing for improved optical interconnection," *ZTE Communications*, vol. 18, no. 2, pp. 57 - 73, Jun. 2020. doi: 10.12142/ZTECOM.202002008.

1 Introduction

In the past decade, the data traffic has been explosively increasing due to applications such as 4K/8K display, cloud computing, 4G/5G and augmented reality/virtual reality (AR/VR), urgently driving the demand of high-capacity data communications. Typically, the very severe data traffic for communication and interaction occurs in data centers with single-lane data rate over 100 Gbit/s. For this scenario, traditional electrical interconnects find its bottlenecks in the perspective of power consumption, available bandwidth and implementation density. In contrast, optical approach exhibits great advantages of high capacity, high density, and perfect robustness to ambient environment as well as improved energy efficiency. With these excellent features, optical intensity-modulation and direct-detection (IM-DD) solution is adopted by IEEE 802.3bs Task Force, for over 100 Gbit/s interconnects with distance ranging from 100 m to 10 km[1]. The ongoing trend of standardization is utilizing advanced modulation formats and suitable optical devices for IM-DD systems.

In the perspective of modulation formats, advanced solutions enable improved spectrum efficiency (SE) for short-reach application including pulse amplitude modulation (PAM)[2-4], quadrature amplitude modulation (QAM)[5-7], orthogonal frequency division multiplexing (OFDM)[8-10], discrete multi-tone (DMT) modulation[11-14] and carrier-less amplitude phase (CAP) modulation[15-18], as shown in **Fig. 1**. PAM, which exhibits the advantages of simplicity and easy synchronization is currently the most suitable candidate for IM-DD optical interconnects with a distance below 10 km. By comparison, QAM and OFDM based on orthogonal multiplexing supporting coherent detection with improved receiver sensitivity, are applicable for interconnection distance over 10 km. DMT is one special solution of channel-adaptive OFDM, by loading modulations with different bit numbers on individual subcarriers with reference to the channel's signal-to-noise-ratio (SNR) response. Consequently, DMT performs better in channels constrained and fluctuated by bandwidth. While CAP improves its SE by means of Nyquist shaping, it is more bandwidth efficient than PAM. Moreover, the finite impulse response (FIR) filters can be implemented on digital circuits with ignorable latency (related to FIR's tap number), making CAP more promising for short-reach optical interconnection.

To get the best use of these formats, hardware parts of an IM-DD system should be carefully selected to find the best

This work was supported by National Natural Science Foundation of China (NSFC) under Grant Nos. 61935011, 61875124 and 61875049.

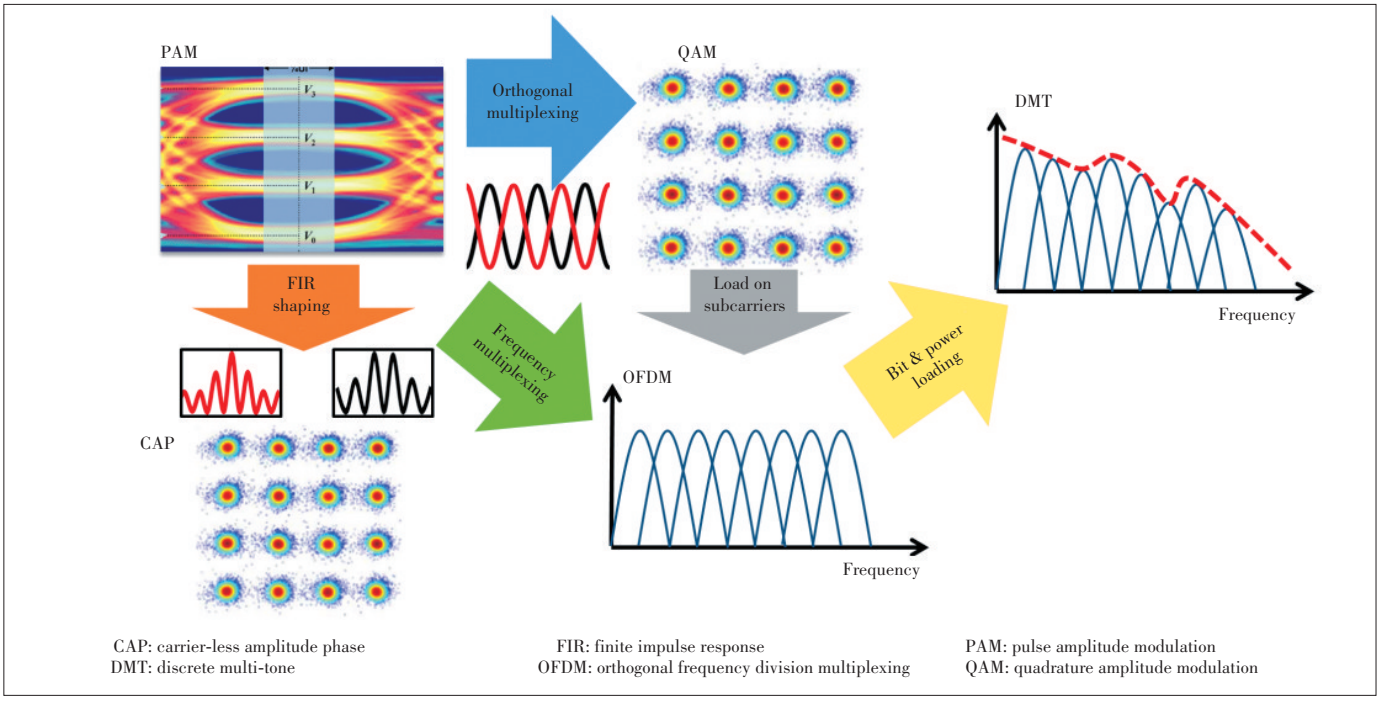

▲**Figure 1. Advanced modulation formats for short-reach optical interconnections.**

trade-off among available bandwidth, fabrication density and power consumption. For interconnection distance below 1 km, vertically cavity surface emitting laser (VCSEL) combined with multi-mode fiber (MMF) is the most power efficient solution, because power cost is mostly concerned in this circumstance. While for longer interconnection distance where severe dispersion bothers, single-mode fiber (SMF) transmission assisted with silicon modulator exhibits simultaneous advantages of large-scale integration and high capacity. Typically, silicon micro-ring modulator (Si-MRM) has the attractive feature of compact footprint, high modulation speed, and low energy consumption, thus it is quite suitable for this scenario.

Consequently, above-mentioned modulation formats, combined with suitable optical hardware, can improve the capacity whilst maintaining the simplicity and reliability. However, advanced modulation formats always show comparably weak robustness to noise and signal distortion during modulation and transmission. In detail, at the same baud rate, PAM-4 suffers severer eye closure than on-off keying (OOK) due to the bandwidth limitation[19]. More level numbers (constellation numbers for QAM) of PAM lead to more sensitivity to SNR limitation. Furthermore, modulation nonlinearity always occurs, which severely degrades signal quality for PAM-4 (much severer for PAM-8). As for VCSEL-based links, modulation nonlinearity is mainly caused by the nonlinear light-current (LI) response of VCSEL, as shown in **Fig. 2a**[20]. Moreover, due to the temperature-sensitive feature of VCSEL, the corresponding LI response can be easily deteriorated by temperature change, leading to more difficulties for linear operation. While for Si-MRM based SMF links, modulation nonlinearity is mainly induced due to the free carrier dispersion effect and the Lorentz spectral shape of the Si-MRM[21–22]. A small wavelength drift of MRM's spectra may lead to severe nonlinearity, as shown in **Fig. 2b**. So for VCSEL and Si-MRM based systems, the modulation nonlinearity is a specific distortion of PAM and other formats. In addition, power cost is also a critical concern for short-reach interconnection. As a result, how to pursue the cost-effective signaling is quite important. Therefore, for short-reach optical interconnection utilizing advanced modulation formats based on VCSEL and Si-MRM, the main issues are: 1) how to improve the performance under limited SNRs; 2) how to mitigate the modulation nonlinearity; 3) how to further enhance the energy efficiency.

At the same time, improved digital signal processing (DSP) technologies have been extensively investigated due to the desire of high-capacity transmission and low power consumption for optical interconnection. Widely known methods such as maximum likelihood sequence estimator (MLSE)[23–25], decision feedback equalizer (DFE)[26–28] and feed-forward equalizer (FFE)[29–30] have been utilized in attempt to improve the system's robustness to inter-symbol interference (ISI).

In this paper, we take a review about the current works as to how to deal with above-mentioned three specific issues by DSP methods for adaptive operation, including our finished and ongoing works as well. This paper is composed of four parts. Section 1 is the introduction of short-reach optical interconnections. Section 2 is DSP methods at the transmitting side, mainly introducing probabilistic shaping. Section 3 is DSP in the receiver, mainly about machine-learning assisted techniques. Section 4 is the conclusions.

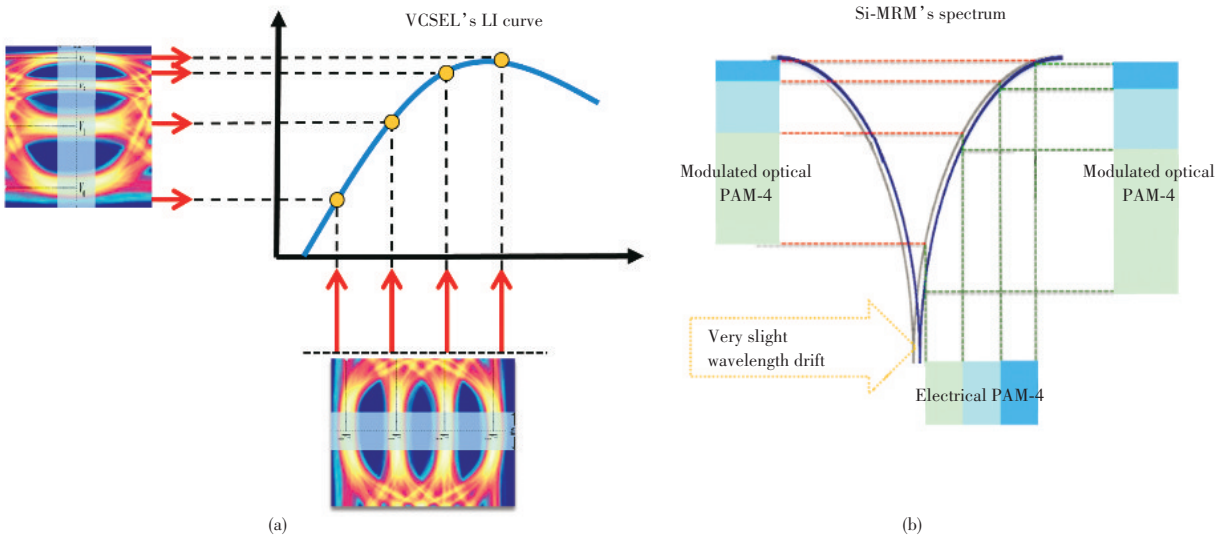

LI: light-current PAM: pulse amplitude modulation Si-MRM: silicon micro-ring modulator VCSEL: vertically cavity surface emitting laser

▲Figure 2. Modulation nonlinearity caused by: (a) nonlinear LI curve of vertically cavity surface emitting laser VCSEL; (b) nonlinear spectra of Si-MRM as well as wavelength drift.

2 Adaptive Probabilistic Shaping at the Transmitter

Very recently, probabilistic shaping (PS) as a coding method has been rapidly developed in the field of coherent optical communications[31 - 39]. PS can bring two benefits simultaneously: 1) improved achievable information rate (AIR) at the low SNR condition[40]; 2) reduced average power due to PS when voltage of peak-to-peak (Vpp) is fixed[41]. Consequently, PS is a quite useful approach to improve the transmission performance at the SNR-constrained condition, and enhance the energy efficiency at the same time. In the field of direct detection system, the theoretical AIR gain of 0.19 bit at 16.2 dB SNR has been reported by using the exponential distributions of 6 level PAM signals, and a corresponding experiment is presented by external modulation at 1550 nm for single mode fiber transmission[42]. Meanwhile, an entropy loading scheme of DMT is reported to fit channel SNR response based on PS[43 - 45]. In Ref. [44], the entropy loading is employed after water-filling algorithm to get rid of extra power reallocation for coherent optical system. Because the subcarriers' power is previously adapted to water filling, only limited numbers of shaped distribution are demonstrated. In Ref. [45], an entropy-loaded DMT without power allocation is proposed by using Maxwell-Boltzmann (MB) distribution in visible light communication system, with an AIR of 204 Mbit/s. However, above-stated researches do not focus on the short-reach interconnection.

As discussed in the introduction part, VCSEL exhibits excellent features of lower power cost, high fabrication density and large electrical bandwidth. It is quite suitable for short-reach interconnections applications. Generally, the SNR and bandwidth for VCSEL-MMF links are more limited compared with coherent systems which require high SNR for high-level QAM and large bandwidth for achieving large capacity. It can thus be expected that PS coding will lead to improved AIR which is particularly desired for the VCSEL-MMF links. Most non-uniform distributions (such as the Maxwell-Boltzmann distribution and the exponential distribution) require distribution matchers and complex code words to code independent and identically distributed sequences into non-uniform ones with the desired distributions[36], and the induced complexity is not suitable for the cost-sensitive short reach optical interconnections. As a result, the objective of this section is to investigate the power-efficient and low-complexity PS methods for cost-effective VCSEL-MMF optical interconnections.

2.1 Dyadic Probabilistic Shaping for PAM

Dyadic PS is advantageous with simple implementation, which makes it particularly suitable for the cost-effective short reach applications. Moreover, PS coding can reallocate majority distributions to lower levels (near direct current) of the PAM signal, resulting in reduced average power along with improved energy efficiency. The VCSEL-MMF solution is currently dominating the sub-hundred-meter-distance optical interconnections with very large volume. The SNR and bandwidth for VCSEL-MMF links are particularly constrained. Therefore, we believe the proposed dyadic PS method is an opportune solution for the cost-sensitive VCSEL-MMF links due to its simplicity of coding with shaping gain and power reduction. To obtain dyadic distributions, binary mapping of M bits generates symbols with probability of 2-M. However, such

variable-length coding will induce synchronization complexity at the receiver, when the noisy sequences are processed. One practical solution is to insert ambiguity bits to maintain the code words in the same length. The probability distributions of PAM-4 and PAM-8, and the shaped signals are shown in **Fig. 3**.

Then the theoretical AIR values are calculated for evaluating the performance of above distributions. As shown in **Fig. 4a,** AIR goes saturated along with the increase of SNR. The saturated AIR (maximum AIR) is reduced after dyadic PS, compared with the uniform distribution. However, at a certain SNR region, such as 10.3 – 16.57 dB for PAM-4 and 16.6 – 25.5 dB for PAM-8 (P'X), AIR values after dyadic PS become larger compared with those before shaping. It indicates that dyadic PS can increase the AIR of PAM-*N* system at the condition of constrained SNR. The zoom-in plot in **Fig. 4b** shows the AIR performances of the PAM-*N* modulations for SNR ranging from 14 dB to 24 dB. For PAM-4, the SNR requirement is reduced by 0.61 dB to achieve the 20% soft decision-forward error correction (SD-FEC) threshold (AIR=1.6 bit/symbol) after dyadic PS. As for PAM-8, 1.08 dB and 1.74 dB, SNR gains are obtained by dyadic PS to achieve 2.4 bit/symbol AIR, by using distributions of P'X and P''X respectively.

Experiments have been carried out directly for PAM-8 modulation over a VCSEL-MMF optical interconnection link to verify the performance of dyadic PS. Due to the inserted ambiguity bits of PS PAM-8, the code rate is 13/16. Consequently, to maintain the same data rate of 60 Gbit/s, the symbol rate of PS PAM-8 increases to 25 Gbaud (30 Gbaud to achieve the net rate of 75 Gbit/s). The optical back-to-back (B2B) eye-diagrams of the 60 Gbit/s and 75 Gbit/s PAM-8, before and after PS, are plotted in **Fig. 5**. The opening of the eye-

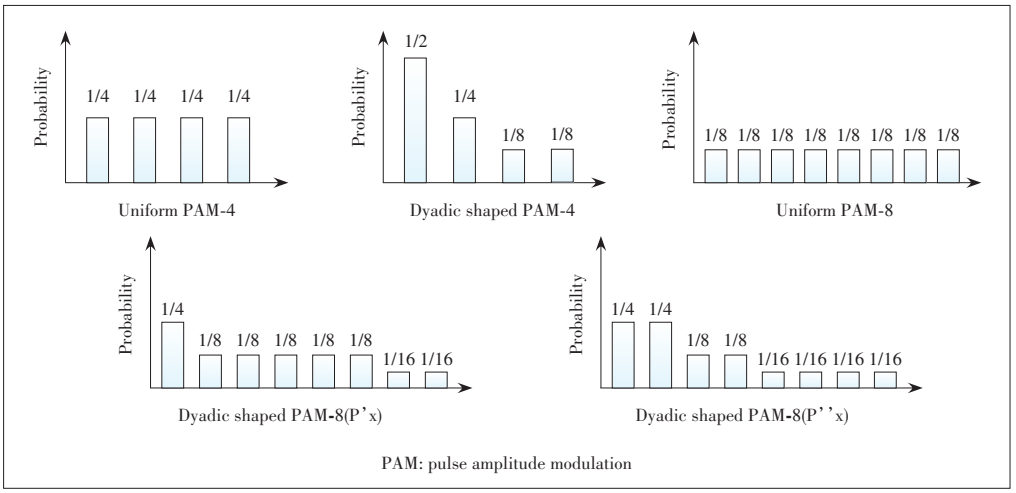

▲**Figure 3. Dyadic probability distributions of PAM-4, PAM-8, dyadic shaped PAM-4, dyadic shaped PAM-8 (P'X) and dyadic shaped PAM-8(P''X).**

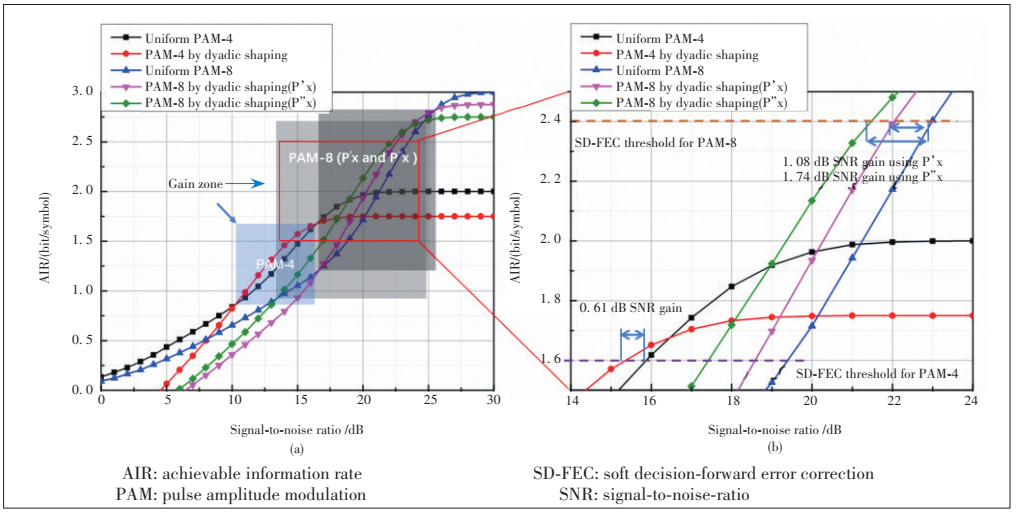

▲**Figure 4. AIR curves for PAM-4 and PAM-8(a) with and (b) without dyadic PS (probabilistic shaping).**

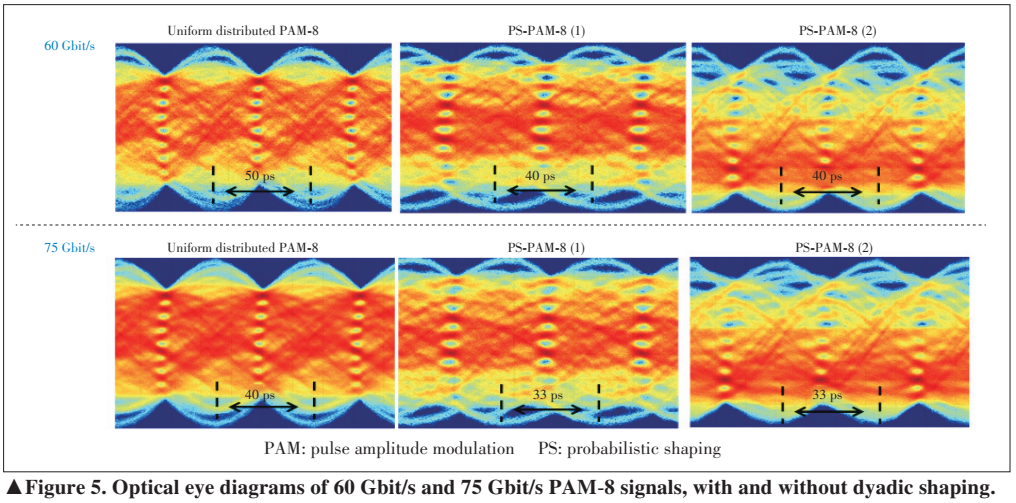

▲**Figure 5. Optical eye diagrams of 60 Gbit/s and 75 Gbit/s PAM-8 signals, with and without dyadic shaping.**

diagrams has been improved (the sub-eye-diagrams are clearer with larger eye-height and eye-width) compared with that before PS. The bit error ratio (BER) curves of 75 Gbit/s PAM-8 signals are plotted in **Fig. 6**. Due to the increased symbol rates, the limited bandwidth of the optical channel shrinks the signal spectrum more severely. Consequently, the shaping gain of dyadic PS PAM-8 signals is smaller than theoretical one under this circumstance. Despite this, 0.88 dB and 0.3 dB SNR gain is obtained for optical B2B case and 100 m OM3 fiber transmission at 75 Gbit/s.

2.2. Maxwell-Boltzmann and Dyadic Probabilistic Shaping for DMT

The dyadic shaping has been demonstrated in PAM system. While for most practical IM-DD channels, frequency response is usually uneven with SNR fluctuating in the frequency domain due to fiber dispersion. A DMT modulation is proposed as a way to address this problem, by loading modulations with different bit-numbers on individual subcarriers with reference to the channel's SNR response. However, for conventional DMT, the constellations of individual subcarriers are all equal-probability distributed. Here we demonstrate a frequency-resolved adaptive probabilistic shaping method which refers to channel frequency response, for the 112 Gbit/s DMT-modulated IM-DD optical interconnection system. The continuously bit (in terms of entropy) loading is realized by adapted probability distributions, allowing for better fitting to channel frequency response with simultaneous shaping gain.

The proposed bit-loading metrology for probabilistic shaping-discrete multi-tone (PS-DMT) is illustrated in **Fig. 7.** A rounding-up function is performed for B_i to obtain standard constellations for QAM-N noted as B_i*, and N denotes the constellation number. The corresponding bit-to-symbol mapping is performed as $N = 2^{B_i^*}$. Finally, the optimization problem must be solved to search for the distribution of the 1D PAM signals. The optimization object is to obtain the 1D probability distribution with entropy that is most close to $B_i/2$. These distributions are subject to the MB equation $P = e^{-|x|}$ with a variable. In addition, the MB distributions require large-length block to perform PS coding. Here, we use Geometric Huffman Coding (GHC) to match dyadic distributions to MB ones.

The experiment investigation of 112 Gbit/s optical interconnection is carried out using a VCSEL-MMF link. In the optical B2B link case, the bit-loading results for conventional DMT are shown as the red points in **Fig. 8,** while the bit-loading results for the proposed PS-DMT (MB) scheme are plotted as blue points. Entropies of dyadic shaped PS-DMT are marked by blue lines. The adapted SNR response by power reallocation is measured by sending multi-tone quadrature phase shift keying (QPSK) signals with reallocated power, plotted as pink line in Fig. 8. In fact, the adapted response is not precisely matched to loaded bit numbers for conventional DMT. Fortunately, PS-DMT can get rid of this deviation, by directly adapting entropies to channel response. The corresponding optimized distributions for 12th and 66th subcarriers are shown in Fig. 8a, respectively. It should be noted here that it is usually impractical to implement the ideal bit-loading number (typically a decimal) perfectly. Only specific PS coding can be

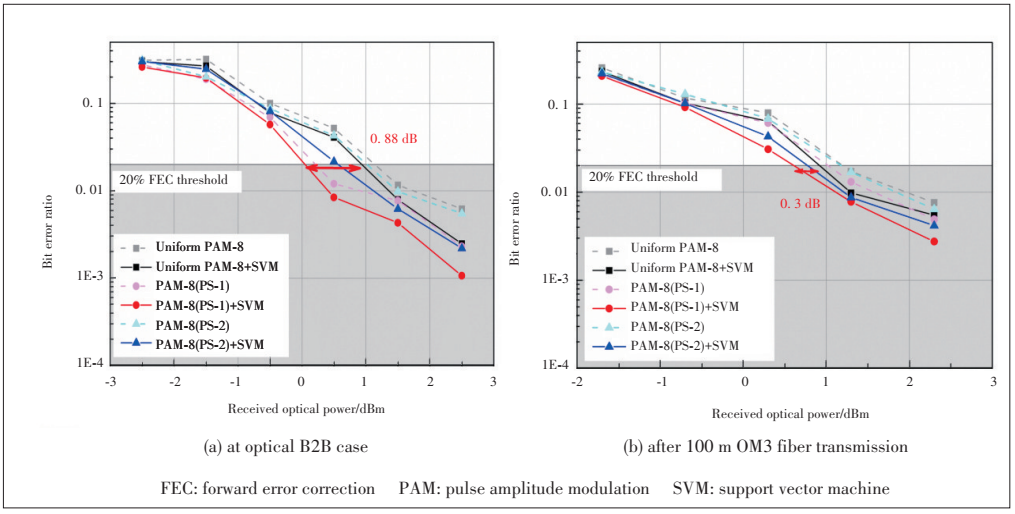

▲**Figure 6. Bit error ratio (BER) curves of 75 Gbit/s PAM-8 signals.**

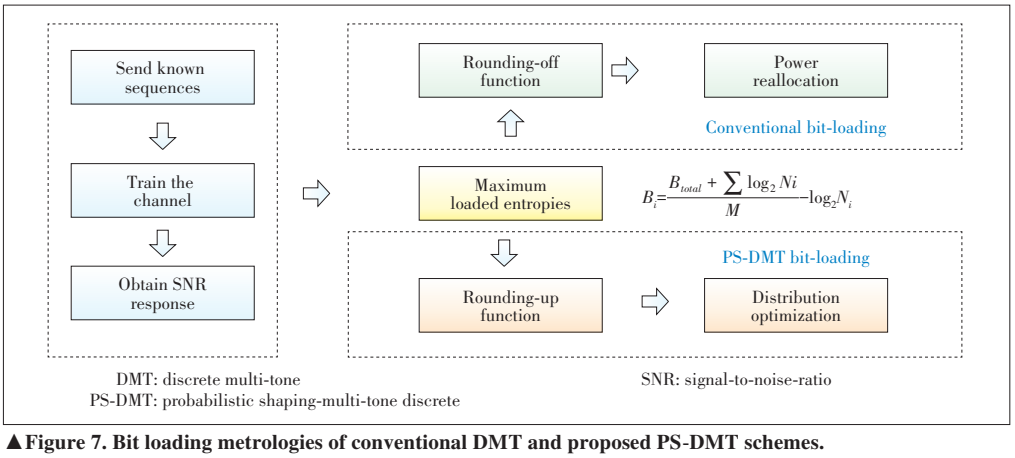

▲**Figure 7. Bit loading metrologies of conventional DMT and proposed PS-DMT schemes.**

used to approach it maximally. A distribution matcher (DM) using dyadic distributions is used to approach the ideal bit-loading number approximately. The matched dyadic distributions are also inserted in Fig. 8b.

With an optical power of 3.5 dBm for the optical B2B case, the demodulated constellations for both DMT and PS-DMT at the receiver are plotted as shown in **Fig. 9**. Constellations are drawn for two selected typical subcarriers (12th and 66th). In addition, the right side of Fig. 9 shows the constellations of these typical subcarriers after 100 m OM3 fiber transmission with a received optical power of 3.3 dBm. The improvement in the signal quality related to the PS shaping gain can be observed visually by the clearer constellations that appear after PS when compared with those obtained before PS. It can also be seen that the constellations become clearer after PS. This occurs because the Euclidean distances between the symbols are broadened, with more symbols being gathered at the center, when the average power is fixed. After 100 m OM3 fiber transmission, however, the channel-efficient bandwidth is reduced, and more bits are loaded on the lower-frequency subcarriers. As a result, the constellations are much noisier after the 100 m transmission. Additionally, the shaped constellations are obviously clearer, with more bits being allocated at their centers. However, after transmission, the received constellations always rotate because of the fluctuating phase response.

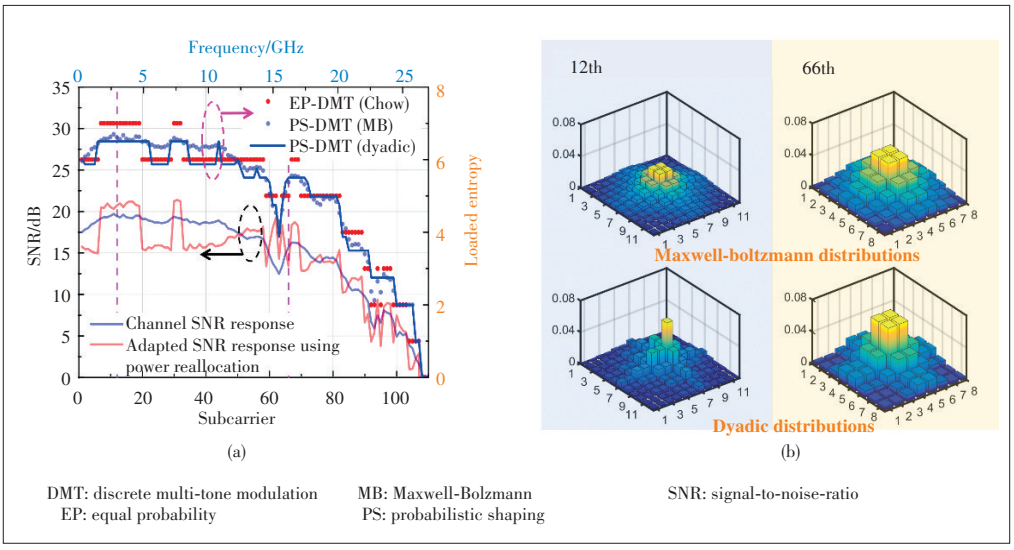

▲**Figure 8. Experimental bit loading results for DMT and PS-DMT in the optical B2B case: (a) bit-loading results for conventional DMT, PS-DMT and PS-DMT (dyadic); (b) shaped probability distributions of two typical subcarriers (22th and 66th subcarriers) for PS-DMT.**

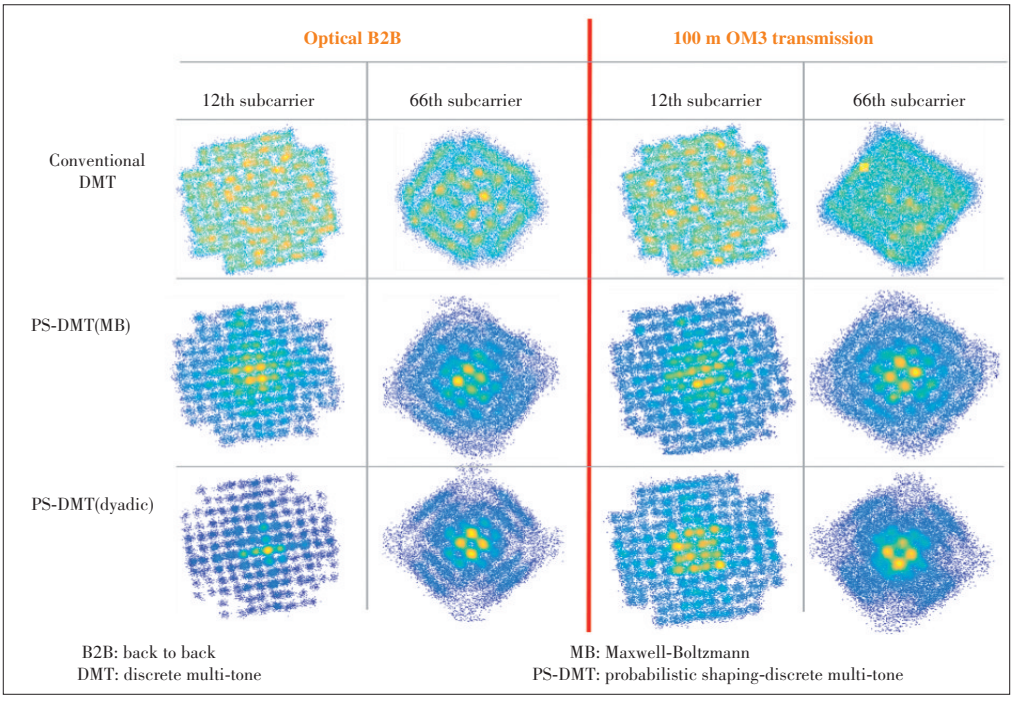

▲**Figure 9. Constellations of 12th and 66th subcarriers for optical B2B case (3.5 dBm received power) and after 100 m OM3 fiber transmission (3.3 dBm received power).**

The total general mutual information (GMI) values of a DMT symbol are then calculated with varying received optical power values, as shown in **Fig. 10**. Without noise and signal distortion, the total GMI value equals to the loaded bit numbers of a DMT symbol (552 in this experiment). As the optical power decreases, the total GMI also decreases rapidly because of the low SNR. In the optical B2B case, with an optical power of more than 1 dBm, the SNR is sufficient to keep the GMI value stable. However, for optical powers below 1 dBm, any reduction in the SNR also reduces the GMI values of high-density constellations, which results in sharply reduced GMI values. After 100 m OM3 fiber transmission, more bits are allocated to the lower-frequency subcarriers because the bandwidth is more constrained. In this case, when the optical power decreases, the higher-density constellations with larger bit-loading numbers suffer greater

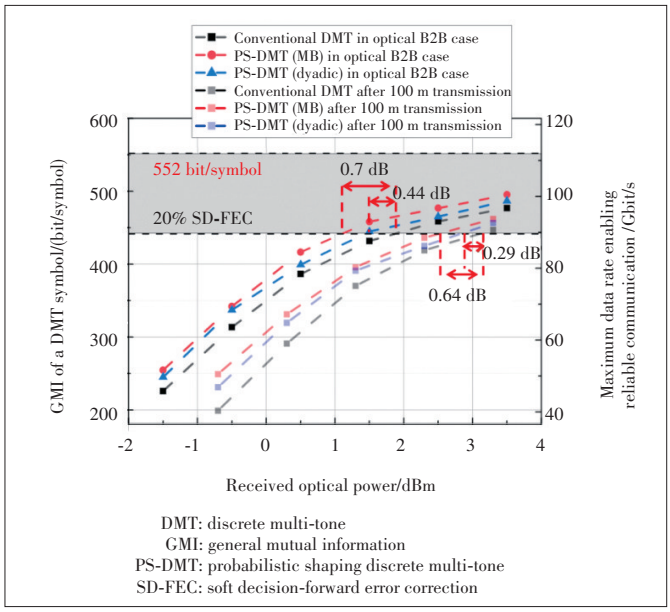

▲Figure 10. Experimental GMI values and data rate of reliable communication under various received optical powers.

GMI reduction than those in the optical B2B case. To enable error-free signaling at 112 Gbit/s with 20% SD-FEC, power sensitivity gains of 0.7 dB and 0.64 dB can be obtained for the optical B2B case and the 100 m OM3 fiber transmission case, assisted by PS-DMT (MB). For PS-DMT (dyadic), power sensitivity gains are 0.44 dB and 0.29 dB for optical B2B and 100 m transmission. The corresponding enabling data rate for reliable transmission is calculated by the multiplication of GMI value and the symbol rate.

3 Advanced DSP at the Receiver

DSP embedded at the receiver side mainly includes post equalization, decoding and decision. Equalization aims to recover signals from severe ISI and noise. Decoding is always performed to correct bit errors, combined with pre-coding at the transmitter. Then advanced decision methods are in attempts to obtain reduced BER when nonlinear distortion occurs. Apart from the tradition DSP methods like FFE, DFE and MLSE, machine-leaning assisted DSP recently exhibits improved performance. It can be used for formats identification[46 - 47], system monitoring[48 - 49] as well as optical signal receiving. For signal receiving technologies, machine learning can be utilized in equalization and decision for achieving distinguished performance[50 - 55].

For the equalization part, the progressive support vector machine (SVM) algorithm has been applied to reduce nonlinear inter-subcarrier intermixing in coherent optical OFDM[50]. Moreover, artificial neural network can also be embedded in equalization part, to reduce the error vector magnitude (EVM) of constellations[51]. As for the decision part, machine-learning techniques can adaptively learn the optimal decision line for obtaining the lowest BER[52 - 55]. Related works mainly focus on QAM signals, and utilized SVMs to mitigate the phase noise. Therefore, the ML method is quite a viable solution for solving the nonlinearity problem (Kerr nonlinearity or modulation nonlinearity), which is the key issue in optical communications. For short reach optical communications, modulation nonlinearity becomes very serious for advanced modulation formats like QAM, PAM, CAP and DMT which are all sensitive to the linearity, both for direct modulation of VCSEL and for external modulation of silicon modulator.

3.1 SVM for QAM Decision

High-order QAM is an efficient format for increasing the transmission capacity due to its high spectral efficiency. However, such dense constellations make QAM signals very sensitive to nonlinear distortion. When nonlinear distortion bothers, the decision boundary can no longer be a simple straight line for obtaining a better BER performance. To deal with it, we propose several SVM multi-classification methods to obtain adaptive nonlinear decision boundary for QAM decision, based on one versus rest (OvR) and binary tree (BT) structure. Different classification methods have different performance in terms of classification precision and complexity.

The OvR SVM is to generate a hyper plane between a class of samples and the remaining multi-class samples, and to realize multi-class recognition. Therefore, if it is an N classification problem, then N SVMs (N>2) are required to perform classification. For example, if the OvR SVM scheme is used for deciding QAM-8 sequences, the data are divided into two categories for every SVM classifier. Consequently, it requires eight SVMs to decide eight symbols of QAM-8 signal.

On the other hand, BT structure can be used to reduce the number of SVM classifier for QAM-N signal decision. Starting from the root node, the category is divided into two subclasses, and then the two subclasses are further divided, until the subclass contains only one category. Here, we employ three different BT-based SVM classification schemes including the binary encoding (BE), the constellation rows (CR) and columns, and the in-phase and quadrature components (IQC). Since the QAM constellation mapping can be realized through binary encoding, the multi-classification based on BE can be performed to decide every bit information of QAM-N. **Fig. 11a** shows the training model for 16-QAM, where the hyper plane generated by each SVM does not take all the training set data into consideration, which can effectively reduce the training time. When testing, only four SVMs is required to perform decision, as shown in **Fig. 11b**. Another BT-based decision scheme can be realized by rows-and-columns classification. Most of the constellations are rectangle, except for 32-QAM, 128-QAM, etc., thus the label feature according to rows and columns is reasonable. Besides, according to the IQC, the QAM signal can be regarded as two PAM signals, which means splitting a binary tree training model into two binary trees to reduce the SVM numbers.

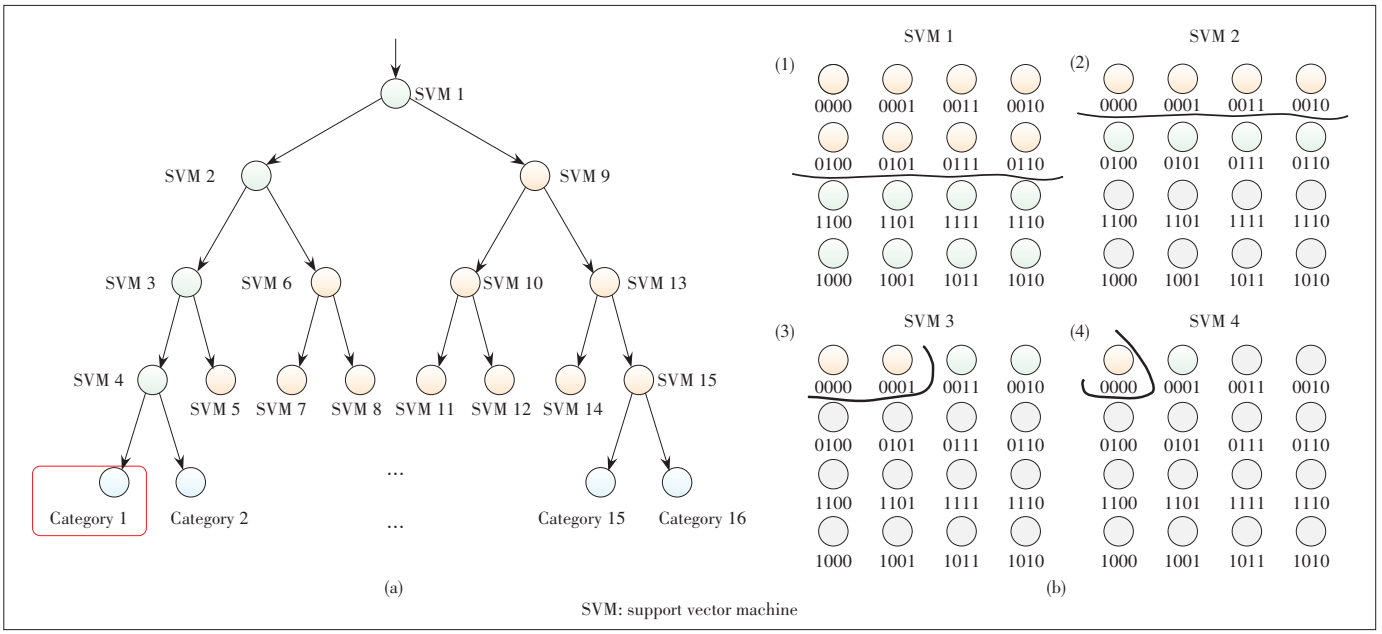

▲**Figure 11. (a) The training model of SVM based on binary-tree structure; (b) a schematic diagram of the hyper plane generated by node SVM for the training processing of category 1.**

To experimentally evaluate above-mentioned decision methods, DMT signaling is realized on the SMF-based optical interconnects system. DMT symbol is composed of different QAM modulations in frequency domain, thus the decision methods can be investigated for analyzing individual subcarriers. Corresponding experimental setup is illustrated in **Fig. 12**. An arbitrary waveform generator (AWG) is used to generate the DMT signal with 54 GSa/s. The laser operates at 1 550 nm followed with external modulation by a Mach-Zehnder-Modulator (MZ-M). The optical signal is coupled into 10 km standard single-mode fiber (SSMF) for transmission. A photodetector (PD) with 22 GHz bandwidth is used for detecting the transmitted optical signal from the SSMF. A digital storage oscilloscope (DSO) (Keysight Z592A) with 59 GHz bandwidth is used to sample the signal with a sampling rate of 160 GSa/s for the offline DSP. Based on the BER results, complexity comparison among the four decision methods is shown in **Table 1**.

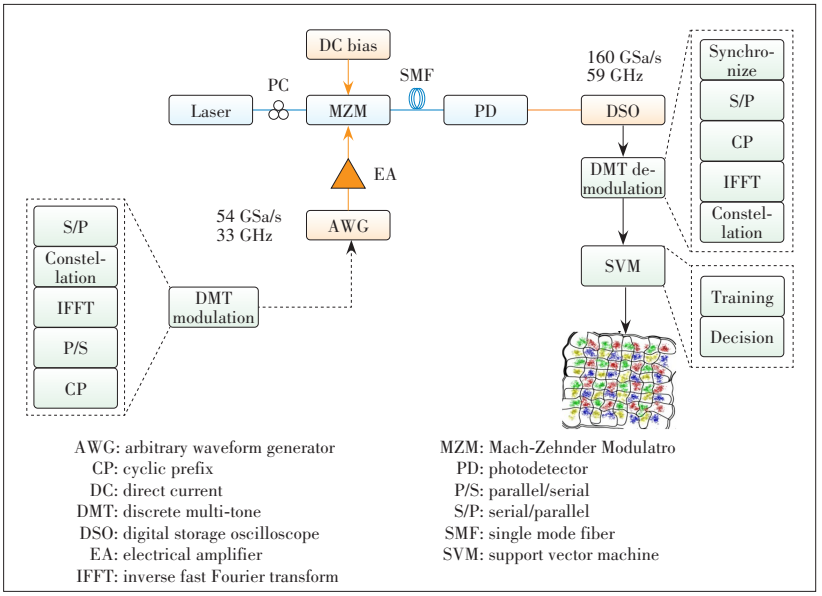

▲**Figure 12. Experimental setup of QAM decision based on SVM classification methods.**

▼**Table 1. Complexity comparison for different SVM-based decision schemes**

Complexity	OvR	BE	CR	IQC
SVM number for training	2 294	2 177	2 177	804
Support vector number ($\times 10^5$)	11.61	1.367	1.376	1.997
Average SVM number for testing	2 294	492	492	492

BE: binary encoding
IQC: in-phase and quadrature components
OvR: one versus rest
CR: constellation rows

In terms of complexity during training and decision processes, OvR-based SVM is the worst, with about 6 to 8 times the number of support vectors to others. While, the number of SVMs for decision is similar for the remaining three methods. In detail, the IQ-based decision method only requires about one-third of the SVM number compared with other methods, which benefits simple implementation. It is worth mentioning that one should carefully evaluate the requirement regarding different application scenarios (particularly different modulationing formats and different nonlinear distortions) when choosing a specific classification method for SVM machine learning detection.

3.2 SVM for PAM Decision

As discussed above, BT-based SVM decision can efficiently improve transmission performance, along with considerable complexity. In this section, BT-based SVM decision is employed to mitigate modulation nonlinearity in PAM-modulated systems, specifically including VCSEL-MMF as well as Si-MRM optical links. In detail, as for VCSEL-based links, modulation nonlinearity is mainly caused by the nonlinear LI response of VCSEL. While for SMF links based on Si-MRM, modulation nonlinearity is mainly induced due to the Lorentz spectral shape of the Si-MRM. When processing nonlinearly-distorted PAM signals, SVM-based decision scheme can generate adaptive boundaries for the obtained improved decision performance.

3.2.1 Optical Interconnection Link Based on VCSEL-MMF

To evaluate the performance of binary tree-support vector machines (BT-SVM) decision for PAM signals, the experiment based on VCSEL-MMF system has been carried out at a bit rates of 60 Gbit/s for PAM-4 and PAM-8. With the received optical power being manually attenuated, BER curves of the PAM-4 and PAM-8 signals are plotted in **Fig. 13**, where 20%-overhead FEC is assumed for investigating the receiver sensitivity. Consequently, there are about 1 dB and 2 dB receiver sensitivity improvements with the use of complete binary tree-support vector machines (CBT-SVMs) classifier, respectively for PAM-4 and PAM-8 signals. Improvement for PAM-8 is clearly better compared with PAM-4 due to its doubled modulation levels, which makes it more sensitive to modulation nonlinearity distortion as we expected.

Moreover, it is essential to quantitatively analyze the machine learning performance of CBT-SVMs classifier for PAM signals under different modulation nonlinearities. **Fig. 14** shows the SVM machine learning performance of CBT-SVMs classifier with the increase of eye-linearity (increase of modulation nonlinearity distortion). Here we use 7% overhead FEC threshold for investigating receiver sensitivity. The sensitivity changes almost linearly with eye-linearity. Smaller power (receiver sensitivity) can be obtained by using BT-SVMs classifier, which has a smaller slope as shown in Fig. 14. The smaller slope means an increased sensitivity gain with the increase of eye-linearity. The very severely distorted eye diagram with an eye-linearity of 1.72 is also presented in Fig. 14. A sensitivity gain of 2.5 dB is obtained by the proposed CBT-SVMs at eye-linearity of 1.72. One can expect larger gain for larger eye-linearity.

3.2.2 Optical Interconnection Link Based on Si-MRM-SMF

Besides VCSEL-based optical link, the Si-MRM will induce severe modulation nonlinearity. Si-MRM exhibits the attractive features of compact footprint, high modulation speed, and low energy consumption. However, the high Q factor of the Si-MRM makes it very sensitive to resonance drift, which means it may cause serious damage to the signal. Here, we model a PAM-4 modulated optical interconnections system, with different Si-MRM resonator wavelengths as shown in **Fig. 15**. 100 Gbit/s PAM-4 signals are generated with a bandwidth of 50 GHz. The

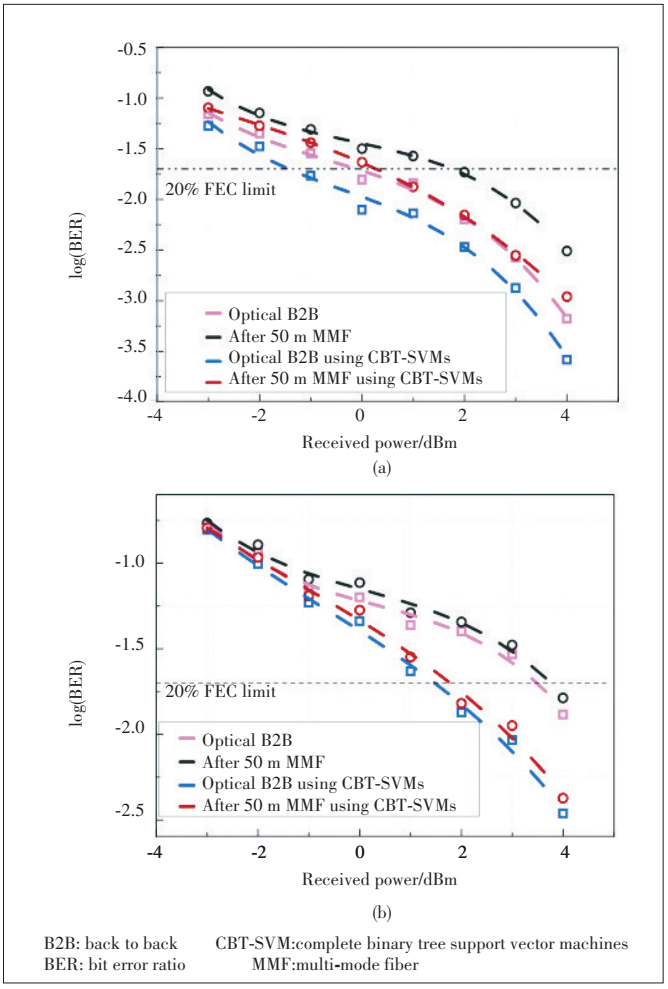

▲Figure 13. BER curves by using conventional hard decision and proposed CBT-SVM for (a) PAM-4; (b) PAM-8.

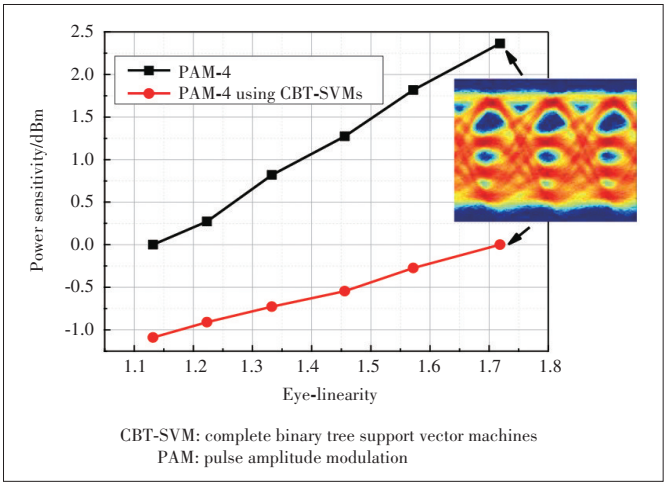

▲Figure 14. Optical power sensitivity versus different eye-linearity value by using conventional hard decision and proposed CBT-SVM.

bandwidths of digital-to-analogue-converter and analogue-to-digital-converter (DAC/ADC) as well as optical link in the simulation system are set at 40 GHz. A PD with 1 A/W sensitivity is used to detect the optical signal. The thermal noise of the PD is set to be 10^{e}-12 A/$\sqrt{\text{Hz}}$.

In the simulation, PAM-4 signals are biased at 0.7 V, and Vpp of PAM-4 signals is 1 V. The Si-MRM linear operation range is very narrow, and the temperature drift will affect the Si-MRM transmission which leads to the degradation of the PAM-4 modulation. To quantitatively analyze the influence of wavelength drift for the PAM-4 signals, we use a term of level-deviation (LD).

Fig. 16 denotes the LD as a function of the Si-MRM resonant wavelength, which refers to the wavelength drift. It can be seen that even very slight wavelength drift will lead to deteriorated LD. **Fig. 17** shows the sensitivity gain as a function of LD. The power sensitivity gain means the reduction of the received power requirement for achieving error free (assuming 7% overhead FEC) by using CBT-SVMs with respect to hard decision. The black line in Fig. 17 represents the forward wavelength drift and the red one refers to the reverse wavelength drift. From Fig. 17, generally, the sensitivity gain increases along with the increase of the LD (absolute value) which means larger gain due to machine learning detection for larger modulation nonlinearity distortion. The largest sensitivity gain is about 2.7 dB. Fig. 17 also gives the sensitivity of CBT-SVMs at different LDs as shown by the blue and yellow dash-dot curves. The sensitivity powers for all the cases with different LDs are comparably stable with less than 3 dB fluctuation. This also indicates the very useful capability of machine learning detection for stabilized PAM-4 modulation without wavelength drift control at the transmitter side.

3.3 Recurrent Neural Network (RNN) for PAM

For PAM modulated optical interconnections system, another distortion degrading performance is eye skewing. **Fig. 18** illustrates the eye-diagrams of PAM-4 signal before and after VCSEL modulation. The eye-skewing always occurs when the signal is modulated directly on laser. The potential reason behind the skewed eye is the variant rise times with different amplitudes.

Therefore, we propose an RNN-based demodulator to deal with the problem of system performance degradation caused by eye skewing in VCSEL-based PAM system. Compared with other neural network methods, RNN adds a feedback mechanism to the network architecture, which may adaptively learn the skewing during VCSEL modulation. Here, we employ long short-term memory (LSTM) scheme to decode eye-skewing PAM-4 signal. The structure of LSTM is indicated in **Fig. 19**. LSTM is split into four parts: unit status, forgetting gates, input gates, and output gates. The unit state of LSTM is primarily used to transmit information from the previous unit to the next unit. The main function of the forgetting gate is to receive the information of the previous neuron and the input information of current neuron, and at the same time determine how

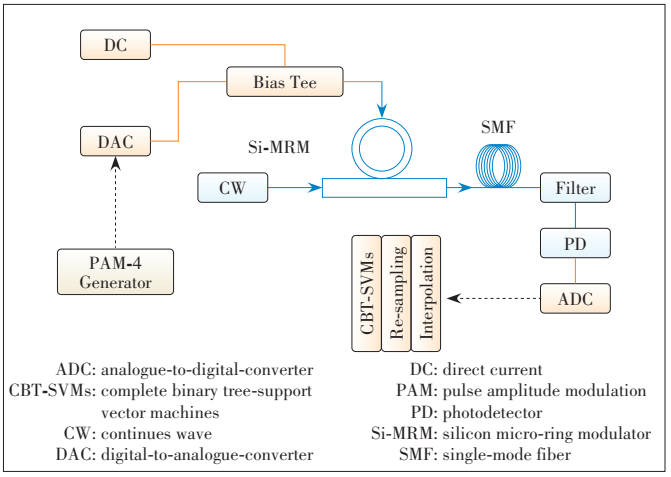

▲ **Figure 15. Simulation setup of Si-MRM based optical interconnects system.**

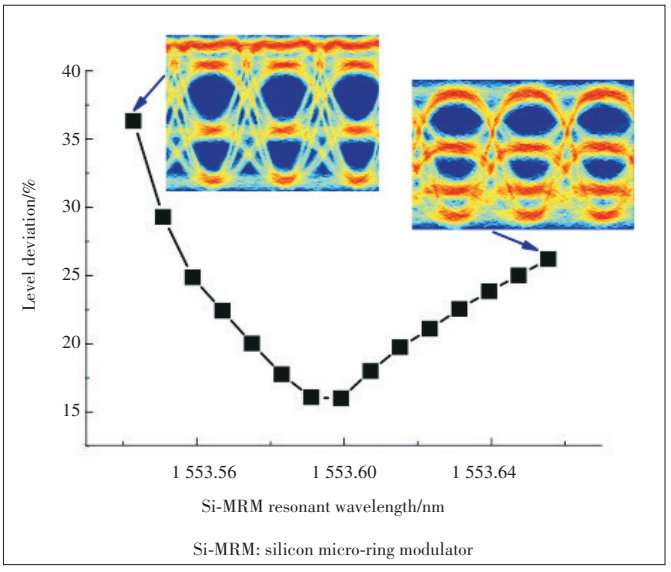

▲ **Figure 16. The level-deviation curve as a function of the wavelength drift. Inserted pictures are the eye diagrams at different wavelengths.**

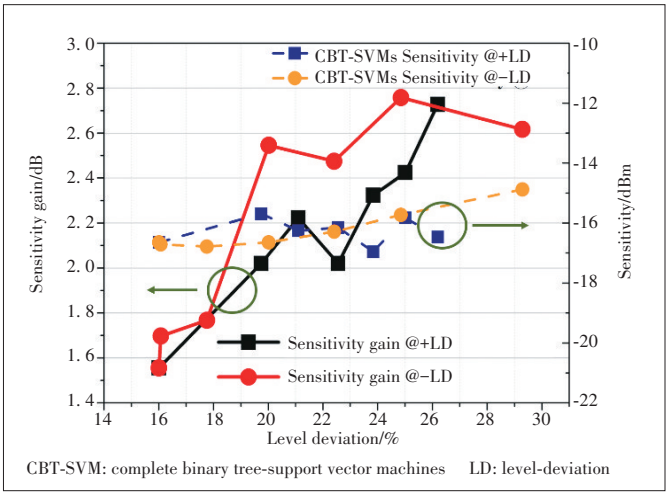

▲ **Figure 17. Sensitivity gain (solid curves) and receiver sensitivity power (dashed curves) for the machine learning detection at different LDs.**

much the state of the last neuron is forgotten. The function of the input gate is mainly to cooperate with a tanh function to control the input of new information. The output gate activates the neuron state information through the tanh function to obtain the output result. The sigmoid in the structure produces coefficients that control the amount of information filtered. In this way, RNN completes the function of information transmission, forgetting, and memory.

In this experiment, the RNN we used was a 10-layer neural network. The number of data for this trial was 20 000. We used 20% as the training set for the neural network, and the remaining 80% was used to test the performance of the RNN in the system.

Fig. 20 shows the BER curves of PAM-4 by using conventional hard decision (HD), CBT-SVM decision and LSTM. BER curves by using conventional HD and CBT-SVM exhibit a linear increasing trend as the optical power decreases, but RNN shows different phenomena around 1 dBm optical power. For RNN by means of sequence mining, the BER performance of the system is stabilized. In general, compared with hard decisions, RNN can bring about 2 dB power sensitivity improvement to the system, slightly better than CBT-SVMs.

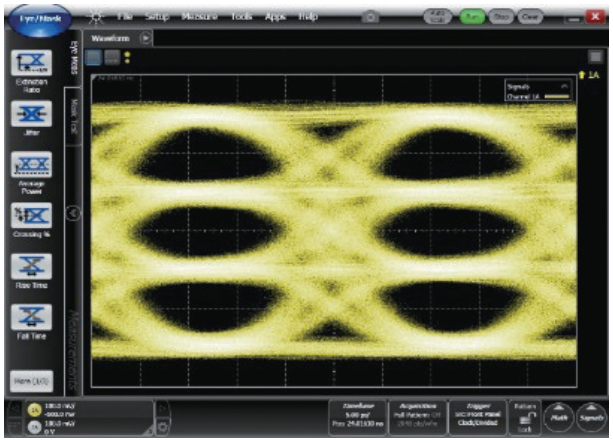

(a) before vertically cavity surface emitting laser (VCSEL) modulation

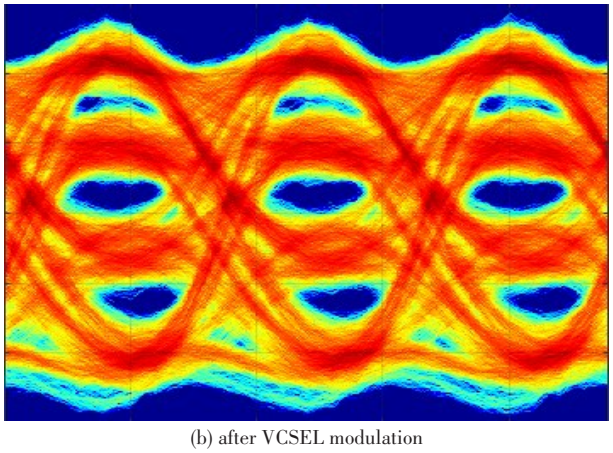

(b) after VCSEL modulation

▲Figure 18. PAM-4 eye-diagram.

3.4 K-Means Clustering for Soft Decision in PAM System

Above mentioned classification methods require training the system through prior-known sequences, resulting in enhanced complexity. To deal with it, a K-means machine learning method assisted signal receiver including both equalization and soft decision is proposed for VCSEL-based PAM-4 optical interconnection. Mean values and noise variances of four levels can be obtained through K-means clustering, without training using prior-known sequences. According to the learned level means, least mean square (LMS) equalization based on the corresponding level-adapted sequences is expected with improved performance. Moreover, based on learned level means and variances, the precision of log-likelihood ratio (LLR) estimation can be enhanced, which leads to the improved performance of soft decision (SD).

The schematic diagram of proposed receiver is plotted as **Fig. 21**. K-means clustering is employed after resampling, to adaptively learn the mean values and noise variances for individual levels, denoted as L_n and σ_n. The upper blue box is the

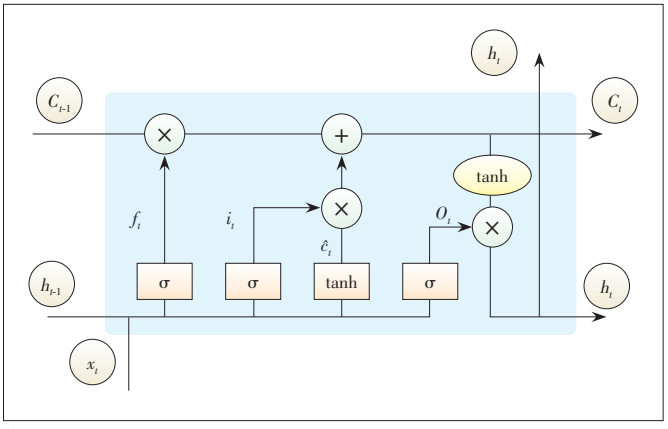

▲Figure 19. Long short-term memory.

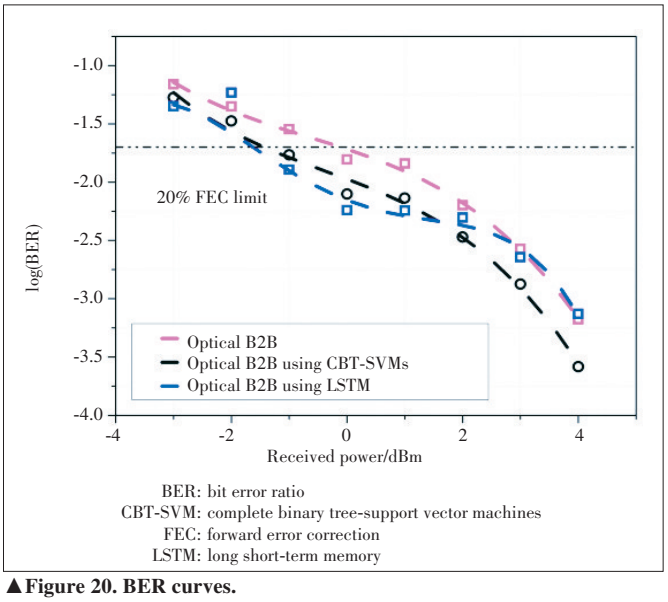

▲Figure 20. BER curves.

equalization part. Tap coefficients are trained through LMS process. Different from conventional LMS, the levels of training sequence are altered adaptively based on learned level means through K-means approach. The lower box is the decision part. With learned level L_n (n=1, 2, 3, 4) and noise variances σ_n, the corresponding LLRs can be calculated. Because it takes level nonlinearity (affecting L_n) and level-dependent noise (affecting σ_n) into consideration, the proposed SD is expected with improved decision precision.

Experiments have been carried out for PAM-4 modulation over a VCSEL-MMF optical interconnection link to verify the performance of the proposed K-means adaptive receiver. To realize 90 Gbit/s and 100 Gbit/s PAM-4 signaling, the sampling rate of AWG is set at 45 Gsa/s and 50 Gsa/s, respectively. The DC bias current is fixed at 15 mA in the experiment. To process the PAM-4 sequences, the sampled signals by DSO have to be re-sampled to 1 sample/symbol. Then the samples are sent into LMS for equalization, and the normalized errors are recorded for every interaction. Error convergence curves for 90 Gbit/s and 100 Gbit/s PAM-4 in optical B2B case are shown in **Figs. 22a** and **22b** respectively, with received optical power of 3 dBm. The residual errors are mainly induced by random noise and residual ISI. And after 100 m transmission, residual errors are higher than the case of optical B2B. It can also be seen that, for K-means LMS (red line), errors converge faster than conventional LMS (blue line). Because for conventional LMS, the levels are mismatched between training sequences and received samples, which deteriorates the convergence performance. This result indicates that lower numbers of interaction can be achieved for K-means LMS.

The eye-diagrams of original sequences, equalized ones as well as LLRs are depicted in **Fig. 23**. It can be seen that 90 Gbit/s PAM-4 in optical B2B case shows clearer eyes than others, which is because less ISI occurs in this circumstance. While for

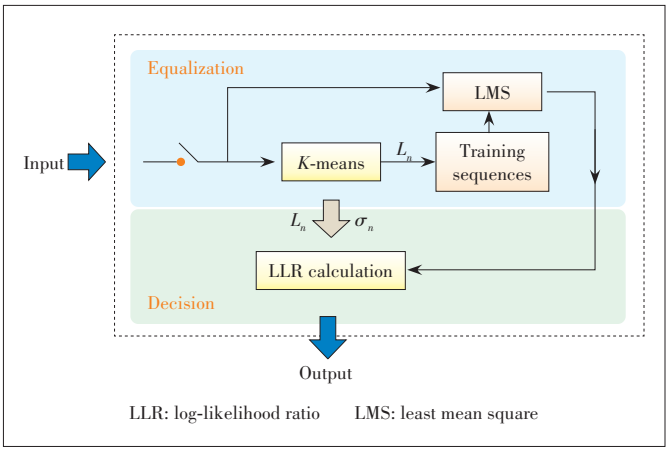

▲ **Figure 21. Proposed K-means receiver including equalization and soft decision.**

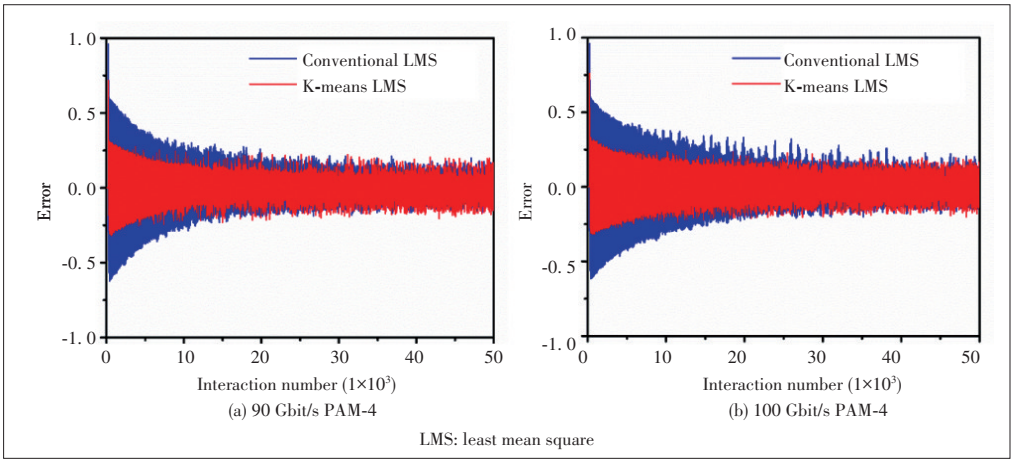

▲**Figure 22. LMS errors during interaction for optical B2B case.**

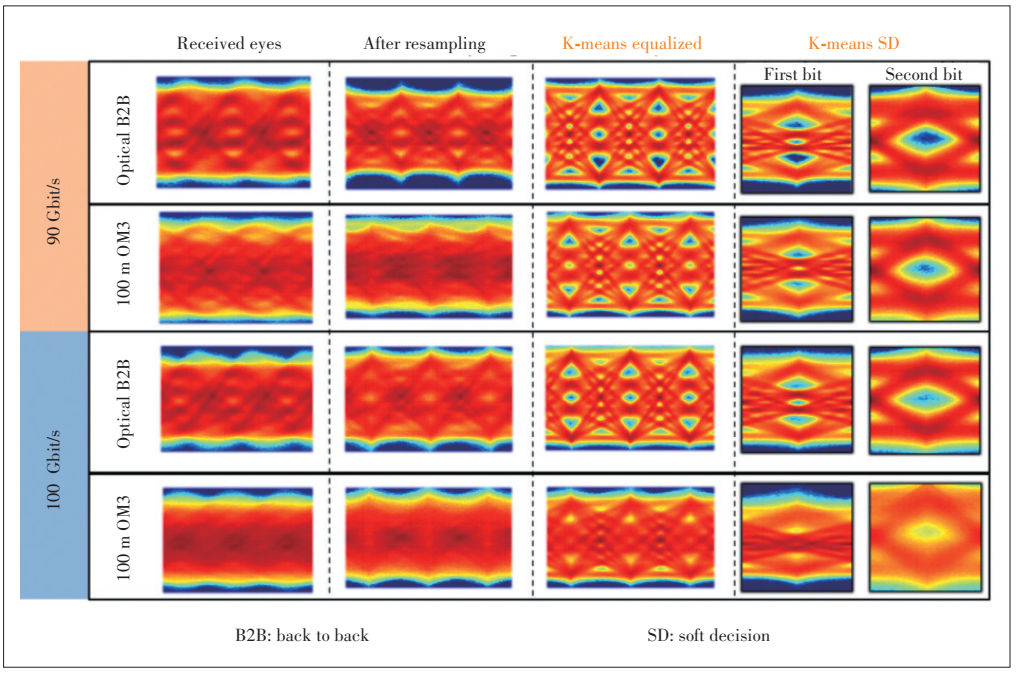

▲**Figure 23. Results of K-means equalization and SD for 90 Gbit/s and 100 Gbit/s PAM-4.**

100 Gbit/s signaling after 100 m OM3 fiber transmission, the eye severely closes with undistinguished four levels. Resampling is performed to obtain 1 sample/symbol sequences, whose eyes are depicted in the second column in Fig. 9. By using K-means equalization, the corresponding eyes are opened obviously, with observable four levels, as shown in the third column. While in the case of 100 Gbit/s and 100 m transmission, the corresponding eye is still noisy, which is because the residual ISI cannot be effectively eliminated. At the fourth column, the two LLR tributaries are demonstrated by means of eye diagram.

3.5 K-Nearest Neighbor (K-NN) for CAP Decision

Apart from PAM, CAP also shows weak tolerance to modulation nonlinearity. Modulation nonlinearity mainly results in irregular constellations for CAP. Consequently, conventional hard decision with the straight decision line cannot obtain considerable BER without considering the modulation nonlinearity. Here, we experimentally investigate the machine learning for nonlinearity mitigation by using K-NN algorithm in 32 Gbit/s CAP system. The basic principle of K-NN algorithm can be intuitively understood from **Fig. 24** (right picture). Firstly, the training signal has to be sampled, shown as blue scatters in constellation diagram. Then when the signal (red point) is detected, its distances to training signals are required to be calculated. And the shortest K distances with responding training samples are selected, to get the constellation label which contains the majority of these training samples (L3 in Fig. 24). It is intuitive that when linear distortion like Gauss white noise occurs, the K-NN algorithm cannot decrease BER compared with the hard decision. However, when constellation is distorted nonlinearly, K-NN is desired to have better performance than the hard decision. The constellation of 32 Gbit/s CAP signal in optical B2B with received optical power at -2 dBm is shown in **Figs. 25a** and **25b**. And the constellation of CAP after 7 km transmission with the same received power is noisier than B2B case, as shown in **Fig. 25c**.

The algorithm complexity of K-NN mainly comes from the selection of K shortest distances. The BER curves of 32 Gbit/s CAP is shown in **Fig. 26**. The K-NN can reduce BER by more than 20 dB for the optical CAP signal, when signal is mainly distorted nonlinearly. However, after 7 km transmission, the signal quality improvement of K-NN is not so obvious when processing signal with low SNR, which is because signal quality is mainly influenced by linear noise.

3.6 SVM for DMT Carrier-by-Carrier Decision

For DMT modulation, nonlinear distortion behaves differently for different subcarriers due to the different bit allocation and SNR. Consequently, every subcarrier suffers different distortions, even for those subcarriers who are loaded by same-order QAM modulation. Thus, adaptive decision is required to perform for every subcarrier. As mentioned above, the SVM-based decision method has the advantage of adaptive decision boundary. Thus, efficient mitigation of the nonlinear distortion for DMT system can be expected through SVM-assisted carrier-by-carrier decision.

An experiment of 112 Gbit/s DMT signaling is performed on VCSEL-MMF optical link. At transmitting side, bit loading and power reallocation are realized according to channel frequency response. The measured channel responses in the case of optical B2B and 100 m OM3 transmission are plotted in **Fig. 27**, as well as corresponding bit loading results. At the receiving side, demodulation of every subcarrier is performed, as well as SVM decision. Constellations of some typical subcarriers are depicted in **Fig. 28**. A total of 40 320 DMT symbols are sent in the experiment and 20% of the data has been used for training. The decoded signal in binary sequence after

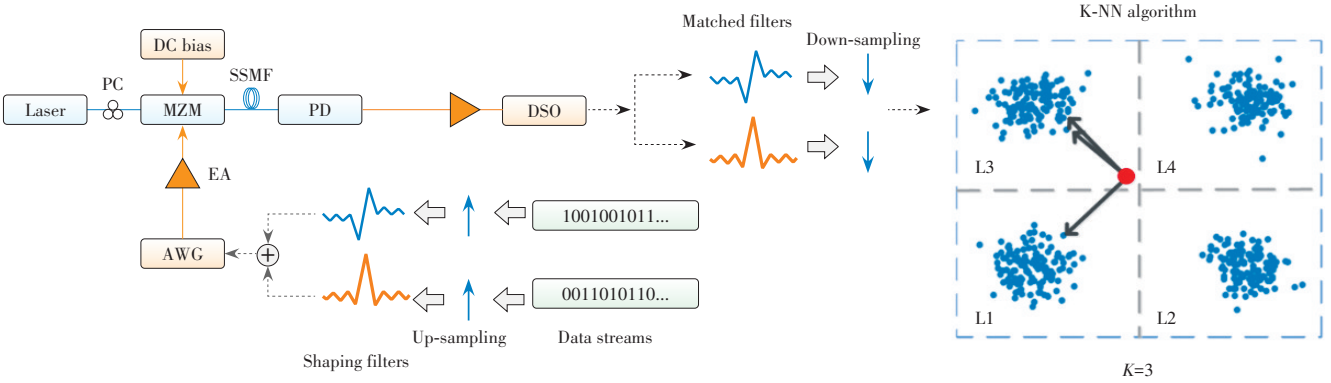

AWG: arbitrary waveform generator
DC: direct current
DSO: digital storage oscilloscope
EA: electrical amplifier
K-NN: K-nearest neighbor
MZM: Mach-Zehnder Modulatro
PC: polarization controller
PD: photodiode
SSMF: standard single mode fiber

▲**Figure 24. Experimental setup of optical carrier-less amplitude phase modulation (CAP) transmission system (left) and principle of K-nearest neighbour algorithm (right).**

de-mapping is then off-line processed for the BER measurement.

Assisted with SVM decision, BER result of DMT system is shown in **Fig. 29**, where significant reduction of BER has been achieved by using SVM detection compared with that using convention detection. Error-free operation has been achieved for B2B case at 7% FEC and 100 m MMF transmission case at 20% FEC.

4 Conclusions

The above mentioned is our current works about advanced DSP methods for optical interconnection systems, mainly including PS coding for transmitter side and machine-learning based DSP for receiver side.

In the perspective of PS, we proposed dyadic shaping for PAM system. Up to 1.74 dB SNR gain can be achieved theoretically by dyadic PS for PAM-8. Proof-of-concept experi-

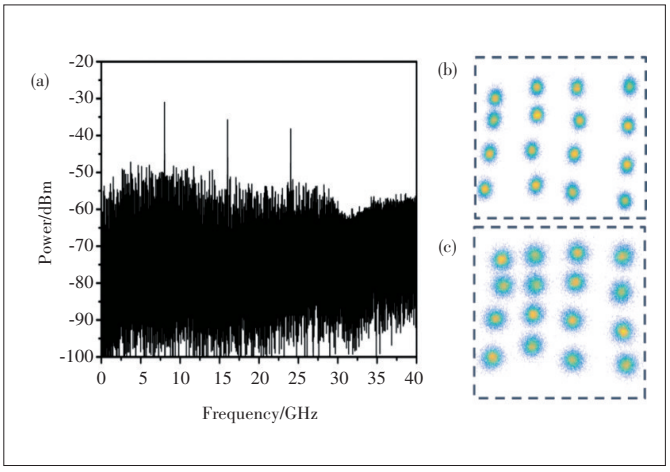

▲**Figure 25. (a) Electrical spectrum of 32 Gbit/s carrier-less optical amplitude phase (CAP) modulation signal; (b) constellation of 32 Gbit/s CAP in optical B2B case; (c) constellation of 32 Gbit/s CAP after 10 km transmission.**

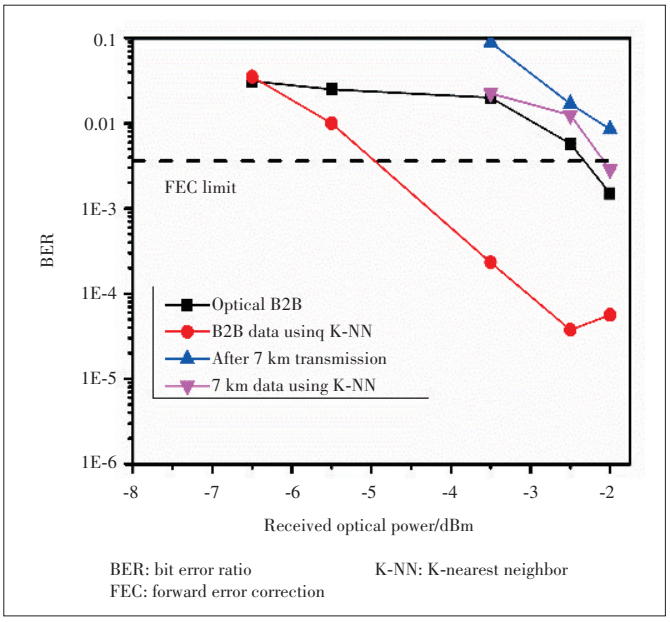

▲**Figure 26. BER curves of 32 Gbit/s optical carrier-less amplitude phase modulation (CAP) by using conventional hard decision and K-NN decision.**

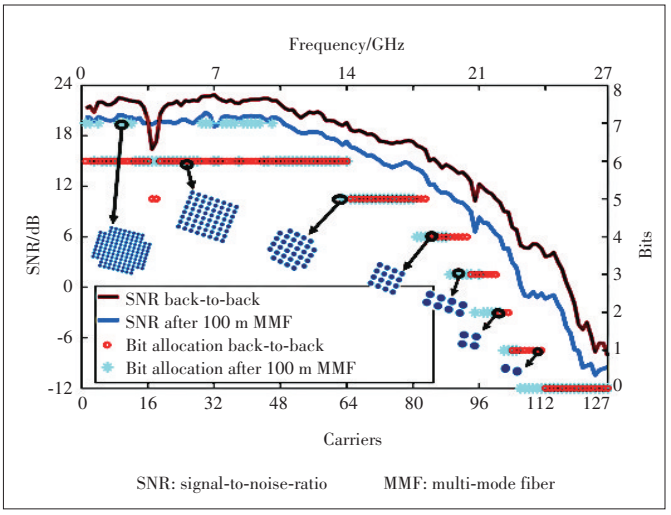

▲**Figure 27. SNR response and bit-allocation of multi-tone modulation (DMT) for back to back (B2B) and 100 m MMF.**

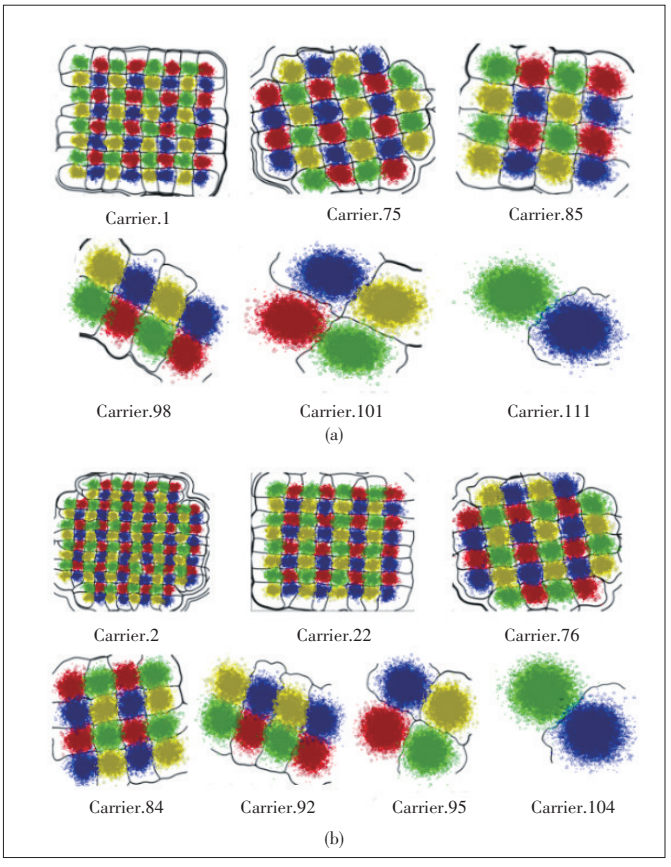

▲**Figure 28. Constellations of some typical subcarriers for multi-tone modulation (DMT) as well as SVM-based decision boundaries for (a) optical B2B case and (b) 100 m MMF transmission.**

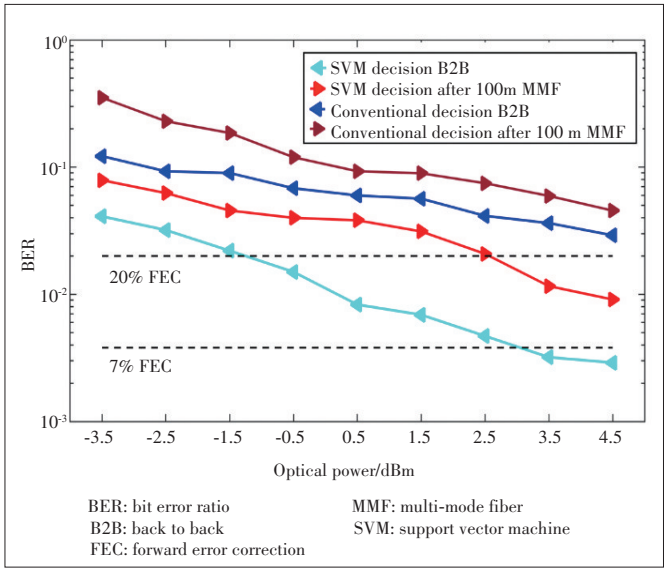

▲Figure 29. BER comparison between using SVM decision and conventional hard decision.

ments have been carried out over a VCSEL-MMF link. Assisted by SVM classifier, 100 m MMF transmission of PS-PAM-8 signals at 75 Gbit/s has been achieved. Energy efficient optical interconnection with 16% reduction of power consumption has been obtained by PS coding. On the other hand, channel-adaptive PS method has been proposed by using DMT modulation, combined with MB shaping. The proposed PS-DMT scheme can significantly improve the signaling capacity since two significant benefits are simultaneously utilized: 1) the shaping gain of PS for carriers with limited SNR; 2) the frequency-resolved continuous entropy loading for better fitting the channel frequency response. Proof-of-concept investigations have been carried out via both simulations and experiments, for MB and dyadic distributions. Data rate improvement of 5.68 Gbit/s was obtained theoretically using the PS-DMT with dyadic distributions. In addition, optical signaling was realized experimentally using a commercial VCSEL at 112 Gbit/s data rate. The 0.44 dB and 0.29 dB power gains have been achieved for optical B2B and 100 m OM3 fiber transmissions, by using dyadic shaping of DMT.

While for DSP methods in the receiver, we mainly employ the machine-learning algorithm to realize improved signal detection. In detail, for QAM signaling, we proposed a SVM multi-classification method to obtain adaptive nonlinear decision boundary. Different classification methods have been evaluated in terms of classification precision and complexity including OvR and BT structure. Among them, the in-phase and quadrature classification method only requires about one-third of the SVM number compared with other methods, which is much simpler for implementation. One should carefully evaluate the requirement regarding different application scenarios (particularly different modulation formats and different nonlinear distortions) when choosing a specific classification method for SVM machine learning detection.

Besides QAM decision, we also use SVM method to mitigate the modulation nonlinearity in PAM-modulated VCSEL-MMF as well as Silicon MRM-SMF optical links. Compared with the published works, we firstly come up with the CBT structure multi-classes SVMs which are more suitable for PAM modulation. For VCSEL-based PAM system, there are about 1 dB and 2 dB receiver sensitivity improvements respectively for PAM-4 and PAM-8 signals with the use of CBT-SVMs classifier. The improvement for PAM-8 is clearly better compared with PAM-4 due to its doubled modulation levels, which makes it more sensitive to modulation nonlinearity distortion as we have expected. For silicon MRM-SMF optical link, the sensitivity versus different LDs are comparably stable with less than 3 dB fluctuation by using proposed CBT-SVM. It indicates the very useful capability of machine learning detection for stabilized PAM-4 modulation without wavelength drift control at the transmitter side. Moreover, we also propose an RNN-based demodulator to mitigate eye skew in VCSEL-PAM system. Compared with other neural networks, RNN adds a feedback mechanism to the network architecture, which can comprehensively consider the association of information before and after the sequence. In detail, compared with hard decisions, RNN can bring about 2 dB power sensitivity improvement to the system, slightly better than CBT-SVMs. Subsequently, a K-means assisted receiver including both equalization and soft decision is proposed for VCSEL-based PAM-4 optical interconnects. Through self-learning of mean values and noise variances of four levels, performance of LMS equalization as well as LLR-based SD has been improved. Besides, we also investigate the performance of machine-learning methods in CAP and DMT system. For CAP system, K-NN based decision is realized for mitigating nonlinear distortion. For DMT system, carrier-by-carrier decision based on SVM is performed, obtained significant reduction of BER.

The above-mentioned are proposed DSP methods and corresponding results. In brief, PS embedded in transmitter (Tx) side and machine-learning decision in receiver (Rx) side are realized. With assistance of such intelligent DSP approach, improved performances in terms of BER and capacity are achieved. Moreover, these methods can be not only utilized for short-reach link, but also extended for long-haul transmission. The challenges for practical application are mainly the cost of complexity with respect to the sensitivity gain. Presently, the complexity is still large and applications for short reach optical interconnection are difficult. However, for long haul, which is not so sensitive to power consumption and cost, complex DSP can be acceptable as long as the gain is large enough. For data center interconnection (DCI) applications ranging from tens of kilometers to hundreds of kilometers, there would be a good balance.

References

[1] XU K, SUN L, XIE Y Q, et al. Transmission of IM/DD signals at 2 μm wavelength using PAM and CAP [J]. IEEE photonics Journal, 2016, 8(5): 1 – 7. DOI: 10.1109/jphot.2016.2602080
[2] KANEDA N, LEE J, CHEN Y K. Nonlinear equalizer for 112-Gb/s SSB-PAM4 in 80-km dispersion uncompensated link [C]//Optical Fiber Communication Conference. Los Angeles, USA, 2017. DOI: 10.1364/ofc.2017.tu2d.5
[3] PANG X D, OZOLINS O, GAIARIN S, et al. Experimental study of 1.55-um EML-based optical IM/DD PAM-4/8 short reach systems [J]. IEEE photonics technology letters, 2017, 29(6): 523 – 526. DOI: 10.1109/lpt.2017.2662948
[4] WINZER P J, GNAUCK A H, DOERR C R, et al. Spectrally efficient long-haul optical networking using 112-Gb/s polarization-multiplexed 16-QAM [J]. Journal of lightwave technology, 2010, 28(4): 547 - 556. DOI: 10.1109/jlt.2009.2031922
[5] KOIZUMI Y, TOYODA K, YOSHIDA M, et al. 1024 QAM (60 Gbit/s) Single-carrier coherent optical transmission over 150 km [J]. Optics express, 2012, 20 (11): 12508 – 12514. DOI:10.1364/oe.20.012508
[6] SEIMETZ M, NOELLE M, PATZAK E. Optical systems with high-order DPSK and star QAM modulation based on interferometric direct detection [J]. Journal of lightwave technology, 2007, 25(6): 1515 – 1530. DOI: 10.1109/jlt.2007.896810
[7] ARMSTRONG J, LOWERY A J. Power efficient optical OFDM [J]. Electronics letters, 2006, 42(6): 370 – 372. DOI:10.1049/el:20063636
[8] YI X W, SHIEH W, TANG Y. Phase estimation for coherent optical OFDM [J]. IEEE photonics technology letters, 2007, 19(12): 919 – 921. DOI: 10.1109/lpt.2007.897572
[9] SHIEH W. PMD-Supported Coherent Optical OFDM Systems [J]. IEEE photonics technology letters, 2007, 19(3): 134 – 136. DOI: 10.1109/lpt.2006.889035
[10] LEE S C J, RANDEL S, BREYER F, et al. PAM-DMT for intensity-modulated and direct-detection optical communication systems [J]. IEEE photonics technology letters, 2009, 21(23): 1749 – 1751. DOI: 10.1109/lpt.2009.2032663
[11] TAKAHARA T, TANAKA T, NISHIHARA M, et al. Discrete multi-tone for 100 Gb/s optical access networks [C]//Optical Fiber Communication Conference. San Francisco, USA, 2014. DOI: 10.1364/OFC.2014.M2I.1
[12] ZHONG K P, ZHOU X, GUI T, et al. Experimental study of PAM-4, CAP-16, and DMT for 100 Gb/s short reach optical transmission systems [J]. Optics express, 2015, 23(2): 1176. DOI: 10.1364/oe.23.001176
[13] NADAL L, SVALUTO MOREOLO M, FABREGA J M, et al. DMT modulation with adaptive loading for high bit rate transmission over directly detected optical channels [J]. Journal of lightwave technology, 2014, 32(21): 4143 – 4153. DOI: 10.1109/jlt.2014.2347418
[14] SUN L, DU J B, HE Z Y. Multiband three-dimensional carrierless amplitude phase modulation for short reach optical communications [J]. Journal of lightwave technology, 2016, 34(13): 3103 – 3109. DOI: 10.1109/jlt.2016.2559783
[15] OLMEDO M I, ZUO T J, JENSEN J B, et al. Multiband carrierless amplitude phase modulation for high capacity optical data links [J]. Journal of lightwave technology, 2014, 32(4): 798 – 804. DOI: 10.1109/jlt.2013.2284926
[16] INGHAM J D, PENTY R V, WHITE I H, et al. 40 Gb/s carrierless amplitude and phase modulation for low-cost optical data communication links[C]//Optical Fiber Communication Conference/National Fiber Optic Engineers Conference. Los Angeles, USA, 2011. DOI: 10.1364/ofc.2011.othz3
[17] SUN L, DU J B, YOU Y, et al. 45-Gbit/s 3D-CAP transmission over a 16-GHz bandwidth SSMF link assisted by wiener filtering [J]. Optics communications, 2017, 389: 118 – 122. DOI: 10.1016/j.optcom.2016.11.055
[18] SZCZERBA K, WESTBERGH P, KAROUT J, et al. 4-PAM for high-speed short-range optical communications [J]. Journal of optical communications and networking, 2012, 4(11): 885 – 894. DOI: 10.1364/jocn.4.000885
[19] MENA P V, MORIKUNI J J, KANG S M, et al. A simple rate-equation-based thermal VCSEL model [J]. Journal of lightwave technology, 1999, 17(5): 865 – 872. DOI: 10.1109/50.762905
[20] WANG L, QIU Y, XIAO X, et al. 24-Gb/s PAM-4 over 150-km SSMF using a driverless silicon microring modulator [C]//Asia Communications and Photonics Conference. Shanghai, China, 2014. DOI: 10.1109/jssc.2006.884342
[21] BOGAERTS W, HEYN P D, VAERENBERGH T V, et al. Silicon microring resonators [J]. Laser & photonics reviews, 2012, 6(1): 47 – 73. DOI: 10.1002/lpor.201100017
[22] RUBSAMEN M, WINZER P J, ESSIAMBRE R J. MLSE receivers for narrowband optical filtering [C]//Optical Fiber Communication Conference & the National Fiber Optic Engineers Conference. Anaheim, USA, 2006. DOI: 10.1109/OFC.2006.215452
[23] STOJANOVIC N, HUANG Y, HAUSKE F N, et al. MLSE-based nonlinearity mitigation for WDM 112 Gbit/s PDM-QPSK transmissions with digital coherent receiver [C]//Optical Fiber Communication Conference. Los Angeles, USA, 2011.DOI: 10.1364/OFC.2011.OWW6
[24] RYLYAKOV A V, SCHOW C L, KASH J A. New ultra-high sensitivityA, low-power optical receiver based on a decision-feedback equalizer [C]//Optical Fiber Communication Conference/National Fiber Optic Engineers Conference, Los Angeles, USA, 2011. DOI: 10.1364/ofc.2011.othp3
[25] BULZACCHELLI J F, MEGHELLI M, RYLOV S V, et al. A 10-Gb/s 5-Tap DFE/4-Tap FFE transceiver in 90-nm CMOS technology [J]. IEEE journal of solid-state circuits, 2006, 41(12): 2885 – 2900. DOI: 10.1109/jssc.2006.884342
[26] ZHOU J, QIAO Y J, YU J J, et al. Interleaved single-carrier frequency-division multiplexing for optical interconnects [J]. Optics express, 2017, 25(9): 10586 – 10596. DOI: 10.1364/oe.25.010586
[27] MAN J W, CHEN W, SONG X L, et al. A Low-cost 100GE optical transceiver module for 2km SMF interconnect with PAM4 modulation[C]//Optical Fiber Communication Conference, San Francisco, USA, 2014. DOI: 10.1364/ofc.2014.m2e.7
[28] KANAZAWA S, YAMAZAKI H, NAKANISHI Y, et al. Transmission of 214-Gbit/s 4-PAM signal using an ultra-broadband lumped-electrode EADFB laser module [C]//Optical Fiber Communication Conference, Anaheim, USA, 2016. DOI: 10.1364/OFC.2016.Th5B.3
[29] VERPLAETSE M, LIN R, KERREBROUCK JVAN, et al. Real-time 100 Gb/s transmission using three-level electrical duobinary modulation for short-reach optical interconnects [J]. Journal of lightwave technology, 2017, 35(7): 1313 – 1319. DOI: 10.1109/jlt.2016.2643778
[30] FEHENBERGER T, LAVERY D, MAHER R, et al. Sensitivity gains by mismatched probabilistic shaping for optical communication systems [J]. IEEE photonics technology letters, 2016, 28(7): 786 – 789. DOI: 10.1109/lpt.2015.2514078
[31] BEYGI L, AGRELL E, KAHN J M, et al. Rate-adaptive coded modulation for fiber-optic communications [J]. Journal of lightwave technology, 2014, 32(2): 333 – 343. DOI: 10.1109/jlt.2013.2285672
[32] BUCHALI F, STEINER F, BÖCHERER G, et al. Rate adaptation and reach increase by probabilistically shaped 64-QAM: an experimental demonstration [J]. Journal of lightwave technology, 2016, 34(7): 1599 – 1609
[33] YANKOV M P, ZIBAR D, LARSEN K J, et al. Constellation shaping for fiber-optic channels with QAM and high spectral efficiency [J]. IEEE photonics technology letters, 2014, 26(23): 2407 – 2410. DOI: 10.1109/lpt.2014.2358274
[34] BÖCHERER G. Capacity-achieving probabilistic shaping for noisy and noiseless channels [EB/OL]. (2012) [2019]. https://www.researchgate.net/publication/268291605_Capacity-Achieving_Probabilistic_Shaping_for_Noisy_and_Noiseless_Channels
[35] BÖCHERER G. On Joint design of probabilistic shaping and forward error correction for optical systems[C]//Optical Fiber Communication Conference, San Diego, USA, 2018. DOI:10.1364/ofc.2018.m4e.1
[36] PAN C P, KSCHISCHANG F R. Probabilistic 16-QAM shaping in WDM systems [J]. Journal of lightwave technology, 2016, 34(18): 4285 – 4292. DOI: 10.1109/jlt.2016.2594296
[37] RENNER J, FEHENBERGER T, YANKOV M P, et al. Experimental comparison of probabilistic shaping methods for unrepeated fiber transmission [J]. Journal of lightwave technology, 2017, 35(22): 4871 – 4879. DOI: 10.1109/jlt.2017.2752243
[38] SEMRAU D, XU T H, SHEVCHENKO N A, et al. Achievable information rates estimates in optically amplified transmission systems using nonlinearity compensation and probabilistic shaping [J]. Optics Letters, 2017, 42(1): 121 – 124. DOI: 10.1364/ol.42.000121
[39] FEHENBERGER T, BÖCHERER G, ALVARADO A, et al. LDPC coded modulation with probabilistic shaping for optical fiber systems [C]//Optical Fiber Communication Conference, Los Angeles, USA, 2015. DOI: 10.1364/ofc.2015.th2a.23
[40] ERIKSSON T A, CHAGNON M, BUCHALI F, et al. 56 Gbaud probabilistically shaped PAM8 for data center interconnects [C]//2017 European Conference on Optical Communication, Gothenburg, Sweden, 2017. DOI: 10.1109/

ecoc.2017.8346148
[41] CHEN X, CHO J, CHANDRASEKHAR S, et al. Single-wavelength, single-polarization, single- photodiode Kramers-Kronig detection of 440-Gb/s entropy-loaded discrete multitone modulation transmitted over 100-km SSMF[C]//2017 IEEE Photonics Conference, Orlando, USA, 2017. DOI: 10.1109/pc2.2017.8283402
[42] CHE D, SHIEH W. Approaching the capacity of colored-SNR optical channels by multicarrier entropy loading [J]. Journal of lightwave technology, 2018, 36 (1): 68 – 78. DOI: 10.1109/jlt.2017.2778290
[43] XIE C H, CHEN Z X, FU S N, et al. Achievable information rate enhancement of visible light communication using probabilistically shaped OFDM modulation [J]. Optics express, 2018, 26(1): 367. DOI: 10.1364/oe.26.000367
[44] KHAN F N, ZHONG K P, AL-ARASHI W H, et al. Modulation format identification in coherent receivers using deep machine learning [J]. IEEE photonics technology letters, 2016, 28(17): 1886 – 1889. DOI: 10.1109/lpt.2016.2574800
[45] WANG D S, ZHANG M, LI Z, et al. Modulation format recognition and OSNR estimation using CNN-based deep learning [J]. IEEE photonics technology letters, 2017, 29(19): 1667 – 1670. DOI: 10.1109/lpt.2017.2742553
[46] THRANE J, WASS J, PIELS M, et al. Machine learning techniques for optical performance monitoring from directly detected PDM-QAM signals [J]. Journal of lightwave technology, 2017, 35(4): 868 – 875. DOI: 10.1109/jlt.2016.2590989
[47] ANDERSON T B, KOWALCZYK A, CLARKE K, et al. Multi impairment monitoring for optical networks [J]. Journal of lightwave technology, 2009, 27(16): 3729 – 3736. DOI: 10.1109/jlt.2009.2025052
[48] GIACOUMIDIS E, MHATLI S, NGUYEN T, et al. Kerr-induced nonlinearity reduction in coherent optical OFDM by low complexity support vector machine regression-based equalization [C]//Optical Fiber Communication Conference, Anaheim, USA, 2016. DOI: 10.1364/ofc.2016.th2a.49
[49] JARAJREH M A, GIACOUMIDIS E, ALDAYA I, et al. Artificial neural network nonlinear equalizer for coherent optical OFDM [J]. IEEE photonics technology letters, 2015, 27(4): 387 – 390. DOI: 10.1109/lpt.2014.2375960
[50] NGUYEN T, MHATLI S, GIACOUMIDIS E, et al. Fiber nonlinearity equalizer based on support vector classification for coherent optical OFDM [J]. IEEE photonics journal, 2016, 8(2): 1 – 9. DOI: 10.1109/jphot.2016.2528886
[51] CHEN G Y, SUN L, XU K, et al. Machine learning of SVM classification utilizing complete binary tree structure for PAM-4/8 optical interconnection [C]//IEEE Optical Interconnects Conference (OI), Santa Fe, USA, 2017. DOI: 10.1109/oic.2017.7965524
[52] WANG D S, ZHANG M, FU M X, et al. Nonlinearity mitigation using a machine learning detector based on k-nearest neighbors [J]. IEEE photonics technology letters, 2016, 28(19): 2102 – 2105. DOI: 10.1109/lpt.2016.2555857
[53] CHEN G Y, DU J B, SUN L, et al. Nonlinear distortion mitigation by machine learning of SVM classification for PAM-4 and PAM-8 modulated optical interconnection [J]. Journal of lightwave technology, 2018, 36(3): 650 – 657. DOI: 10.1109/jlt.2017.2763961
[54] CHEN G Y, DU J B, SUN L, et al. Machine learning adaptive receiver for PAM-4 modulated optical interconnection based on silicon microring modulator [J]. Journal of light wave technology, 2018, 36(18): 4106 – 4113. DOI: 10.1109/jlt.2018.2861710
[55] SUN L, DU J B, HE Z Y. Machine learning for nonlinearity mitigation in CAP modulated optical interconnect system by using k-nearest neighbour algorithm [C]//Asia Communications and Photonics Conference 2016, Wuhan, China, 2016. DOI: 10.1364/acpc.2016.as1b.1

Biographies

SUN Lin received the bachelor's degree in electronic engineering from Sichuan University, China in 2014 and has developed great interest in optical fiber communication field. He is currently working toward the Ph.D. degree at Shanghai Jiao Tong University, China. His research activities and interests include fiber communications, optical signal processing and optical transmission and interconnection.

DU Jiangbing (dujiangbing@sjtu.edu.cn) received the bachelor's degree and the master's degree from the College of Physics and Institute of Modern Optics, Nankai University, China in 2005 and 2008, respectively, and the Ph.D. degree in electronic engineering from the Chinese University of Hong Kong, China, in 2011. He was with Huawei Technologies from 2011 to 2012. He joined Shanghai Jiao Tong University, China as an assistant professor since 2012, and became an associate professor since 2014. He is the author or coauthor of more than 140 journals and conference papers.

HUA Feng received the B.S. and M.S. degrees in optical instrument from Tianjin University, China in 1993 and 1996 respectively. She has worked with ZTE Corporation since 2000. Currently she is a senior engineer focusing on advanced research of cutting-edge optical communication technologies including silicon photonics, spatial division multiplexing and optical backplane. She has more than 10 patents.

TANG Ningfeng received the M.S. degree in testing engineering from Nanjing University of Aeronautics and Astronautics, China, in 1999. He has worked with ZTE Corporation since 1999. Currently he is an architecture engineer focusing on co-packaged optics and optical interconnection equipment. He has more than 10 patents.

HE Zuyuan received B.S. and M.S. degrees in electronic engineering from Shanghai Jiao Tong University, China in 1984 and 1987, respectively, and the Ph.D. degree in optoelectronics from the University of Tokyo, Japan, in 1999. He joined the Nanjing University of Science and Technology, China as a research associate in 1987, and became a lecturer in 1990. From 1995 to 1996, he was a research fellow in University of Tokyo. In 1999, he became a research associate with the University of Tokyo. In 2001, he joined CIENA Corporation, Maryland, USA, as a lead engineer leading the Optical Testing and Optical Process Development Group. He returned to the University of Tokyo as a lecturer in 2003, and became an associate professor in 2005 and a full professor in 2010. He is currently a chair professor of Shanghai Jiao Tong University. His reasearch focuses on optical fiber sensing.